

1 **Title:** The effects of weak selection on neutral diversity at linked sites

2

3 **Author:** Brian Charlesworth

4

5 **Affiliation:**

6 Institute of Evolutionary Biology, School of Biological Sciences, University of Edinburgh,

7 Edinburgh EH9 3FL, United Kingdom

8

9 **Key words:** Associative overdominance, background selection, fixation times, loss times,  
10 neutral variability

11

12 **Running title:** Weak selection and genetic diversity

13

14

15 **Corresponding author:**

16 *Name:* Brian Charlesworth

17 *Address:* Institute of Evolutionary Biology, School of Biological Sciences, Ashworth

18 Laboratories, University of Edinburgh, King's Buildings, Charlotte Auerbach Road,

19 Edinburgh EH9 3FL, UK

20 *Telephone:* +44 131 650 5751

21 *Email:* [Brian.Charlesworth@ed.ac.uk](mailto:Brian.Charlesworth@ed.ac.uk)

22

23

24 **Abstract**

25

26 The effects of selection on variability at linked sites have an important influence on  
27 levels and patterns of within-population variation across the genome. Most theoretical  
28 models of these effects have assumed that selection is sufficiently strong that allele  
29 frequency changes at the loci concerned are largely deterministic. These models have  
30 led to the conclusion that directional selection for selectively favorable mutations, or  
31 against recurrent deleterious mutations, reduces nucleotide site diversity at linked  
32 neutral sites. Recent work has shown, however, that fixations of weakly selected  
33 mutations, accompanied by significant stochastic changes in allele frequencies, can  
34 sometimes cause higher diversity at linked sites when compared with the effects of  
35 fixations of neutral mutations. The present paper extends this work by deriving  
36 approximate expressions for the mean conditional times to fixation and loss of  
37 mutations subject to selection, and analysing the conditions under which selection  
38 increases rather than reduces these times. Simulations are used to examine the relations  
39 between diversity at a neutral site and the fixation and loss times of mutations at a  
40 linked site that is subject to selection. It is shown that the long-term level of neutral  
41 diversity can be increased over the purely neutral value by recurrent fixations and losses  
42 of linked, weakly selected dominant or partially dominant favorable mutations, or linked  
43 recessive or partially recessive deleterious mutations. The results are used to examine  
44 the conditions under which associative overdominance, as opposed to background  
45 selection, is likely to operate.

46

47

## 48 **Introduction**

49 There is now a large body of data showing that the levels of within-population DNA sequence  
50 diversity across the genomes of many organisms are significantly affected by the effects of selection  
51 on sites linked to those under observation, especially in genomic regions or species where  
52 recombination rates are low; for recent reviews, see Cutter and Payseur (2013) and Charlesworth  
53 and Jensen (2021). Interpretations of these observations have mainly focussed on reductions in  
54 variation at linked neutral or nearly neutral sites caused by the spread of selectively favorable  
55 variants (selective sweeps), or the elimination of rare, deleterious mutations (background selection).  
56 The population genetic models used to describe these processes usually assume that selection is  
57 sufficiently strong in relation to genetic drift that deterministic equations are sufficient to describe  
58 the behavior of the sites under selection, except for the initial and final periods of the fixation of  
59 beneficial mutations (reviewed by Charlesworth and Jensen 2021).

60 Interest has, however, recently been revived in the process known as associative  
61 overdominance (Frydenberg 1963; Sved 1968; Ohta 1971; Latter 1998; Pamilo and Palsson 1998,  
62 1999; Wang and Hill 1999; Zhao and Charlesworth 2016; Waller 2021), whereby the level of  
63 diversity at a neutral locus in a diploid population can be enhanced by the presence of linked  
64 deleterious alleles maintained by mutation pressure. Recent theoretical work has shown that this can  
65 happen when the deleterious alleles concerned are sufficiently recessive, and selection is  
66 sufficiently weak in relation to drift (Zhao and Charlesworth 2016). The latter condition requires the  
67 product of the effective size of the population ( $N_e$ ) and the selection coefficient against  
68 homozygotes for a mutation ( $s$ ) to be the order of 1 or less, consistent with previous results from  
69 computer simulations (Latter 1998; Palsson and Pamilo 1999; Wang and Hill 1999). There is  
70 evidence for the operation of associative overdominance (AOD) in both small populations (Latter  
71 1998; Zhao and Charlesworth 2016; Schou et al. 2017; Waller 2021), and in genomic regions with  
72 low recombination, where  $N_e$  is reduced as a result of background selection and selective sweeps  
73 (Becher et al. 2020; Gilbert et al. 2020). In contrast, if the effects of drift on the frequencies of  
74 deleterious alleles are negligible, background selection (BGS) operates, causing a reduction in  
75 variability at linked sites (Charlesworth et al. 1993; Hudson and Kaplan 1995; Nordborg et al.  
76 1996).

77 Under conditions where AOD is acting, deleterious variants at sites under selection are  
78 likely to become fixed as a result of drift, and reverse mutations that increase fitness can eventually  
79 arise and replace them as a result of the joint effects of drift and selection. In the long term, a  
80 population that is constant in size will reach a stochastic equilibrium under the joint effects of drift,

81 mutation and selection, a situation that is similar to that envisaged in the Li-Bulmer model of the  
82 evolution of codon usage bias, which assumes a constant flux of fixations of favorable and  
83 beneficial mutations at sites under selection (Li 1987; Bulmer 1991; McVean and Charlesworth  
84 1999). In order to understand the effects of AOD, it is therefore important to have a model of the  
85 effects of this flux on variability at linked neutral sites.

86 A basis for such a model is provided by the results of Mafessoni and Lachmann (2015) on  
87 the expected times to fixation and loss of new autosomal mutations in a randomly mating  
88 population, and on the effects of fixation events on the patterns of variability at linked neutral loci.  
89 They showed that a weakly selected ( $N_e s$  of order 1), favorable mutation destined for fixation can  
90 have a longer mean time to fixation or loss than a neutral mutation, provided that it is dominant or  
91 partially dominant. The same applies to weakly selected, partially recessive deleterious mutations.  
92 Furthermore, the fixation of a dominant or partially dominant favorable mutation, or of a recessive  
93 or partially recessive deleterious mutation, can enhance variability at a linked neutral site compared  
94 with the effect of fixation of a neutral variant, although variability is still lower than in an  
95 equilibrium population without any selection. These conclusions have been confirmed in the  
96 simulations described by Johri *et al.* (2021); similar situations where fitnesses fluctuate over time  
97 have been studied by Kaushik and Jain (2021). As pointed out by Charlesworth and Jensen (2021),  
98 these results are relevant to the analysis of AOD by Zhao and Charlesworth (2016), who showed  
99 that a neutral locus closely linked to a locus subject to mutation to deleterious alleles can lose  
100 variability more slowly than in the absence of selection, provided that the mutations are recessive or  
101 partially recessive and selection is sufficiently weak relative to the effects of genetic drift.

102 The purpose of this paper is to obtain approximate analytical expressions for the expected  
103 sojourn times of new mutations for the case of weak selection, and to use these to illuminate the  
104 results of Mafessoni and Lachmann (2015) on the fixation and loss of weakly selected mutations.  
105 Computer simulations are used in conjunction with these results to examine the effects of fixations  
106 and losses of weakly selected mutations on variability at linked neutral sites. The results are used to  
107 develop a semi-analytical model of AOD for the case of stochastic equilibrium between mutation,  
108 selection and drift. They also provide a new way of describing BGS, when applied to situations  
109 when selection is so strong in relation to drift that deleterious mutations have a negligible chance of  
110 becoming fixed in the population. The focus is on the case when there is no recombination between  
111 neutral and selected sites, since this gives the clearest signal and allows the causes of the observed  
112 patterns to be analysed without the complications introduced by recombination.

113

## 114 **Material and methods**

### 115 **Simulation methods**

116 To check the accuracy of the diffusion equation results for expected times to fixation or loss (see  
117 the section *Theoretical Results*), a biallelic autosomal locus in a Wright-Fisher population with  
118 constant size  $N$  was modeled, implying that the effective population size  $N_e$  is equal to  $N$ . For a  
119 given simulation run, a single  $A_2$  allele was introduced into the population that was fixed for its  
120 alternative allele  $A_1$ . The mutant allele could be either selectively favorable or deleterious. The  
121 expected change in the frequency  $x$  of  $A_2$  in a given generation for an assigned selection model was  
122 calculated using the standard discrete-generation selection formulation (for details of the model of  
123 selection, see the section *Theoretical Results, Approximate times to fixation and loss of a new*  
124 *mutation*). Binomial sampling using the frequency of  $A_2$  after selection and  $2N$  as parameters was  
125 used to obtain the value of  $x$  in the next generation. Large numbers of replicate simulations were run  
126 in order to obtain the mean times to fixation and loss of  $A_2$ , conditioned on its fixation or loss,  
127 respectively.

128 This procedure was modified in order to calculate the effects of a sweep on pairwise  
129 diversity at a neutral locus with an arbitrary degree of linkage to the selected locus. As described in  
130 Charlesworth (2020a) and Johri et al. (2021), the algorithm of Tajima (1990) was used to calculate  
131 the effects of a sweep on pairwise diversity at a neutral locus with an arbitrary degree of linkage to  
132 a selected locus with two alleles,  $A_1$  and  $A_2$ . Tajima's Equations (27) provide three coupled,  
133 forward-in-time recurrence relations for the expected diversities at the neutral locus for pairs of  
134 haplotypes carrying either  $A_1$  or  $A_2$ , and the divergence between  $A_1$  and  $A_2$  haplotypes. These are  
135 conditioned on a given generation-by-generation trajectory of allele frequencies at the selected  
136 locus, assuming the infinite sites model of mutation and drift (Kimura 1971). In the present study,  
137 there is interest in the effects of both losses and fixations of either deleterious or advantageous  $A_2$   
138 mutations on diversity statistics over the time-course leading to loss or fixation of  $A_2$ , whereas the  
139 previous studies only considered the effects of fixations.

140 For a given simulation run, a single  $A_2$  allele was introduced into the population, with  
141 zero expected pairwise diversity at the associated neutral locus. The initial expected pairwise  
142 diversity among  $A_1$  alleles and divergence between  $A_1$  and  $A_2$  were set equal to those for an  
143 equilibrium population in the absence of selection,  $\theta = 4N_e\mu$ , where  $\mu$  is the neutral mutation  
144 rate. Since only diversities relative to  $\theta$  are of interest here,  $\theta$  was set to 0.001 in order to satisfy  
145 the infinite sites assumption. Equations (27) of Tajima (1990) were applied to the previous value  
146 of the allele frequency in order to obtain the state of the neutral locus in the new generation.

147           The simulation procedure for selection and drift at the selected locus was repeated  
148 generation by generation until  $A_2$  was lost or fixed; if the effect of loss on diversity at the neutral  
149 locus was of interest, only runs in which  $A_2$  was lost were retained, and the value of the pairwise  
150 diversity among  $A_2$  alleles at the time of its loss was determined. Similarly, the effects of  
151 fixations were studied by recording the properties of runs in which  $A_2$  was fixed. Large numbers  
152 of replicate simulations were used (between  $10^4$  and  $10^6$ , depending on the parameter values),  
153 because there is a large amount of variation in the values of the population statistics between  
154 replicate runs.

155           Diversity statistics were obtained in each generation for the three genotypes at the  
156 selected locus. They were measured relative to the equilibrium neutral values, and were thus  
157 equivalent to the mean coalescent times on the timescale of  $2N_e$  generations. The sums of the  
158 pairwise diversity statistics were taken over the whole time course of a loss or fixation, for  $A_1$   
159 versus  $A_1$ ,  $A_1$  versus  $A_2$ , and  $A_2$  versus  $A_2$  haplotypes, as well as the mean over all three of these  
160 comparisons, weighted by their frequencies in the generation in question. In addition, the neutral  
161 diversity of fixed haplotypes at the time of loss or fixation of the mutation was determined.

## 162

### 163 **Numerical integrations**

164           The notation and results described in Ewens (2004, Chapters 4 and 5) are used here, with some  
165 slight modifications. The diffusion equation expressions shown in the Appendix yield the sojourn  
166 time densities at frequency  $x$  of  $A_2$  given an initial frequency  $q$ , which are denoted by  $t^*(x, q)$  and  
167  $t^{**}(x, q)$  for fixations and losses conditioned on fixation or loss, respectively (see Equations A1  
168 and A6). The mean times spent between frequencies  $x$  and  $x + dx$  are given by  $t^*(x, q) dx$  and  
169  $t^{**}(x, q) dx$ , respectively, where  $dx$  is an arbitrarily small increment in  $x$ . The sojourn time  
170 densities involve integrals of the function  $\psi(y)$ , defined by Equation (A1c). For a given value of  
171  $x$ , these integrals can be evaluated for specified upper and lower values of  $y$  by using the series  
172 expansions in Equations (A3). The simplest way to obtain the corresponding conditional mean  
173 times to fixation and loss,  $t^*$  and  $t^{**}$ , for a new mutation with a haploid population size  $N_H$  (see  
174 next section) is to sum the products  $t^*(x, q) / N_H$  and  $t^{**}(x, q) / N_H$  over all values of  $x$  between  $q$   
175 and 1, with  $q = 1/N_H$  (Ewens 2004, p.142).

## 176

### 177 **Theoretical results**

#### 178 **Approximate expected times to fixation and loss of a new mutation**

179 A more general model of selection than that used by Mafessoni and Lachmann (2015) is employed  
180 here, using the notation of Charlesworth (2020a,b). A biallelic locus in a discrete generation,  
181 panmictic population is assumed, with frequencies  $x$  and  $1 - x$  in a given generation of alleles  $A_2$   
182 and  $A_1$ , respectively; the population is initially fixed for  $A_1$ . The new mutation,  $A_2$ , is introduced as  
183 a single copy. To accommodate a general genetic system, the number of haploid genomes at a locus  
184 that are present in the population is denoted by  $N_H$ , so that the initial frequency of  $A_2$  is  $q = 1/N_H$   
185 (Charlesworth 2020a). Selection is sufficiently weak that second-order terms in the selection  
186 coefficient  $s$  for  $A_2A_2$  homozygotes can be neglected ( $s$  is negative if  $A_2A_2$  individuals are at a  
187 selective disadvantage);  $1 + s$  is the fitness of  $A_2A_2$  relative to the fitness of  $A_1A_1$ . The effective  
188 population size is  $N_e$ ; time is measured in units of the coalescent time,  $2N_e$  generations. The scaled  
189 selection coefficient is defined as  $\gamma = 2N_e s$ . Under these assumptions, the rate of change in  
190 frequency of  $A_2$  can be written as:

191

$$192 \quad \Delta x \approx x(1 - x)\gamma(a + bx) \quad (1)$$

193

194 where the coefficients  $a$  and  $b$  depend on the genetic system and breeding system, and higher-order  
195 terms in  $s$  have been neglected (Charlesworth 2020a). In the case of an autosomal locus with  
196 random mating,  $a = h$  and  $b = 1 - 2h$ . Here,  $h$  is the dominance coefficient, such that the fitness of  
197  $A_1A_2$  heterozygotes relative to that of  $A_1A_1$  homozygotes is equal to  $1 + hs$ . This familiar case will  
198 be the focus of this study, but the conclusions can easily be extended to other cases, as described in  
199 Table 1 of Charlesworth (2020a). For example, for an autosomal locus and an inbreeding coefficient  
200  $F$ , we have  $a = F + (1 - F)h$ , and  $b = (1 - F)(1 - 2h)$ . The sign of  $b$  describes whether  $A_2$  is  
201 (partially) dominant or recessive,  $b$  being negative with dominance and positive with recessivity;  $b$   
202 = 0 for a semi-dominant mutation.

203

204 For the present purpose, the main quantities of interest are the sojourn time densities  $t^*(x, q)$   
205 and  $t^{**}(x, q)$  for mutations destined for fixation and loss, respectively, as defined in the Material  
206 and Methods, *Numerical integrations*. These are expressed in units of the coalescent time  $2N_e$ ; the  
207 corresponding absolute times can be obtained by multiplying by  $2N_e$ . When  $A_2$  is initially present as  
208 a single copy, only the situation when  $q \leq x \leq 1$  need be considered; the relevant expressions for  
209  $t^*(x, q)$  and  $t^{**}(x, q)$  are given in the Appendix. Approximations that use only first- and second-  
210 order terms in  $\gamma$  are given by Equations (A5) and (A7), for  $t^*(x, 1/N_H)$  and  $t^{**}(x, 1/N_H)$ ,  
respectively.

211 Equations (A5) and (A7) can be integrated over the interval  $1/N_H \leq x \leq 1$ , yielding  
212 approximate expected conditional times to fixation and loss for a new mutation. We have:

213

$$214 \quad t^* \approx 2 \left\{ 1 - \frac{1}{18} \gamma b - \frac{1}{18} \gamma^2 \left[ a(a+b) + \frac{59}{300} b^2 \right] \right\} \quad (2)$$

215

$$216 \quad t^{**} \approx 2N_H^{-1} \left\{ \ln(N_H) - 1 - \frac{5}{18} \gamma b - \frac{1}{18} \gamma^2 \left[ a(5a + \frac{7}{2}b) + \frac{17}{100} b^2 \right] \right\} \quad (3)$$

217

218

219 For greater accuracy, Euler's constant (0.5772..) should be added to the terms inside the brackets  
220 on the right-hand side of Equation (3), to correct for the difference between the summation and  
221 integration of  $1/x$  (Ewens 2004, p.23). Kaushik and Jain (2021, Equation 9) have independently  
222 derived an approximation similar to Equation (2) for the case of an autosomal locus and random  
223 mating. Their  $H$  corresponds to  $h - 1/2$ ; if terms in  $H^2$  are neglected, their equation is the same as  
224 Equation (2), except for the fact that their expression for  $t^*$  differs by a factor of  $1/2$ , because of their  
225 assumption of a continuous time birth-death process rather than a Wright-Fisher model.

226 The first-order terms in  $\gamma$  in these equations show that when  $b > 0$  ( $h < 0.5$  in the case of  
227 autosomal inheritance), the mean times to fixation and loss of a favorable mutation ( $\gamma > 0$ ) are  
228 reduced below their neutral value, if  $\gamma$  is sufficiently close to 0. These times are increased when  $b <$   
229  $0$  ( $h > 0.5$  with autosomal inheritance). The converse relations hold for the case of a deleterious  
230 mutation ( $\gamma < 0$ ).

231 These results correspond to those of Mafessoni and Lachmann (2015), based on numerical  
232 evaluations of the relevant general equations. Furthermore, when  $b = 0$  (corresponding to semi-  
233 dominance with diploid inheritance),  $t^*$  and  $t^{**}$  are at a maximum with respect to  $\gamma$  when  $\gamma = 0$ , so  
234 that selection on a semi-dominant autosomal mutation (or a semi-dominant mutation with respect to  
235 female fitness with X-linkage) is always associated with a shorter conditional time to fixation or  
236 loss than under neutrality. The results are of interest for the main topic of this paper, because the  
237 flux of mutations between deleterious and favorable alleles at a site is the basis for the analysis of  
238 the long-term effects of weak selection on variability (see the section below on *Relevance to*  
239 *associative overdominance and background selection*). An analysis of the effects of the quadratic  
240 terms in  $\gamma$  on the implications of Equations (2) and (3) is given in the Supplementary File S1,  
241 section 1.

242 A similar treatment can be given for the means of the sum of the diversity  $2x(1-x)$  in each  
243 generation over the paths to fixation or loss of a new mutation ( $H^*$  and  $H^{**}$ , respectively), which



244 are obtained by integrating the product of  $4N_e x(1-x)$  with  $t^*(x, q)$  or  $t^{**}(x, q)$ , respectively, over  $x$   
245 between 0 and 1. The relevant integrations give:

246

$$247 \quad H^* \approx \frac{4}{3}N_e \left\{ 1 - \frac{1}{15}\gamma b - \frac{1}{15}\gamma^2 \left[ a(a+b) + \frac{4}{21}b^2 \right] \right\} \quad (4)$$

248

$$249 \quad H^{**} \approx \frac{8}{3}N_H^{-1}N_e \left\{ 1 - \frac{2}{15}\gamma b - \gamma^2 \left[ \frac{2}{15}a^2 + \frac{1}{10}ab + \frac{1}{210}b^2 \right] \right\} \quad (5)$$

250

251 These expressions show that  $H^*$  and  $H^{**}$  have similar properties to  $t^*$  and  $t^{**}$  with respect to  
252 their dependence on  $b$  when selection is sufficiently weak that first-order terms in  $\gamma$  predominate.  
253 Weak selection with  $\gamma b < 0$  can thus result in an increase in these measures of diversity relative to  
254 neutral expectation, contrary to what is commonly assumed in discussions of molecular variability.  
255 This can happen either when  $\gamma < 0$  and  $b > 0$  (a deleterious, partially recessive or recessive  
256 mutation) or  $\gamma < 0$  and  $b > 0$  (a favorable, partially dominant or dominant mutation).

257 The sojourn time density functions in Equations (A8) and (A9) can be used to find the  
258 corresponding net mean sojourn time between loss or fixation for a new mutation, to an accuracy of  
259 order  $\gamma^2$ :

260

$$261 \quad t \approx 2N_H^{-1} \left\{ \ln(N_H) + 0.5772 + \gamma a - \frac{1}{36}\gamma^2 b(5a+b) \right\} \quad (6)$$

262

263 Similarly, the expected sum of the diversity values over the sojourn of a mutation in the  
264 population before its loss or fixation is approximated by:

265

$$266 \quad H \approx 4N_e N_H^{-1} \left\{ 1 + \frac{1}{3}\gamma a - \frac{1}{18}\gamma^2 b \left( a + \frac{1}{5}b \right) \right\} \quad (7)$$

267

268 With respect to terms of the first order in  $\gamma$ , there is no dependence on  $\gamma b$  of the net mean  
269 sojourn time and net diversity, but they are both increasing functions of  $\gamma a$ . This is consistent with  
270 the classical result for the case of a semi-dominant autosomal mutation with random mating, where  
271  $H$  is an increasing function of  $\gamma$  (Fisher 1930, Figure 3; Kimura 1983, p.44). At first sight, it seems  
272 paradoxical that semi-dominant mutations subject to positive selection should yield a higher net  
273 diversity than neutral mutations during their sojourn in the population. But this is simply a  
274 reflection of the fact that they have a higher chance of establishing themselves in the population,  
275 and hence of contributing to diversity.

276

## 277 Numerical results for conditional times to loss and fixation and net diversity

278 The accuracy of these approximations was checked by comparison with the results of numerical  
279 integrations of the relevant diffusion equation formulae, as described in the Material and Methods  
280 and the Appendix, and by computer simulations of an autosomal locus in a randomly mating  
281 population of size  $N$ , with binomial sampling of post-selection gametes. In this case,  $N_e = N$  and  $N_H$   
282  $= 2N$ . Figure 1 shows the mean fixation time of a new mutation (conditioned on its fixation) for a  
283 range of values of the magnitude of the scaled selection coefficient,  $|\gamma| = 2N_e |s|$ . Both deleterious  
284 mutations ( $s < 0$ ) with dominance coefficient  $h = 0.1$  and favorable mutations with dominance  
285 coefficient  $h = 0.9$  ( $s > 0$ ) were modeled. The values for a neutral mutation, obtained by integration  
286 of the sojourn time density function in the absence of selection with respect to  $x$  between  $1/N_H$  and  
287  $1 - 1/N_H$ , are indicated by the horizontal lines. The results from the numerical integrations of the  
288 sojourn time densities (black curves) are in close agreement with the simulation results (red points)  
289 over the whole range of  $\gamma$  values used here. The approximate values from Equation (2) (blue curves)  
290 are in good agreement with the more exact values for  $|\gamma|$  up to 2 or so, but then tend to overestimate  
291 the fixation times. Nonetheless, the qualitative pattern of an increase in fixation time above the  
292 neutral value as  $|\gamma|$  increases to a value near 2, followed by a decrease, is captured by the  
293 approximation. The more exact results show that the neutral value of  $t^*$  is returned to more quickly,  
294 at  $|\gamma| \approx 3$ , than is indicated by the approximation. As expected from the results of Maruyama (1972)  
295 and Maruyama and Kimura (1974), the curves for favorable and deleterious mutations, with their  
296 complementary values of  $h$ , are identical.

297 Figure 2 shows similar results for the mean times to loss of new mutations, conditioned on  
298 their loss. These are necessarily much smaller than the mean times to fixation, and are also inverse  
299 functions of the population size when measured on the coalescent timescale of  $2N_e$  generations, as  
300 implied by Equation (3). In terms of generations, the loss times are logarithmically increasing  
301 functions of  $N$ , since  $N_e = N$  in the cases shown here. There are noticeable differences between the  
302 results for deleterious and favorable mutations, with the partially deleterious mutations having  
303 longer mean times to loss than the complementary partially dominant favorable mutations (with  
304 dominance coefficient equal to  $1 - h$ , where  $h$  is the value for the corresponding partially recessive  
305 mutations), due to the multiplicands of  $-\gamma^2$  being smaller for the deleterious than the complementary  
306 favorable mutations. Similarly, the deleterious mutations return to the neutral value at larger values  
307 of  $|\gamma|$  than the complementary favorable mutations. The multiplicand of  $-\gamma b$  is larger for losses than  
308 fixations, so that the condition on  $|\gamma|$  for  $t^{**}$  to exceed the neutral value is more liberal for losses

309 than for fixations. However, the second-order terms in both cases are always positive, and  
310 overcome the first-order terms when  $|\gamma|$  is large enough.

311 Similar patterns of behavior are found for the mean sums of the diversities conditioned on  
312 fixations or losses,  $H^*$  and  $H^{**}$ ; examples similar to those in Figures 1 and 2 are shown in Figures  
313 S1 and S2, using the integration and approximate results. As might be expected,  $H^*$  and  $H^{**}$  are  
314 closely correlated with  $t^*$  and  $t^{**}$ , respectively (Figure S3).

315 Figure 3 shows the approximate and integration results for the conditional mean times to  
316 fixation and loss for the whole range of dominance coefficients, with the magnitude of the scaled  
317 selection coefficient  $|\gamma|$  equal to 1 or 2. The approximations (solid curves) agree very well with the  
318 integration results (dashed curves) for both strengths of selection, and are nearly linear in  $h$ . As  
319 expected from Equations 2 and 3, the relationships of the fixation and loss times to  $h$  for the  
320 deleterious and favorable mutations are opposite in direction, with deleterious mutations having  
321 fixation and loss times that decrease with  $h$ , whereas those for favorable mutations increase with  $h$ .  
322 Weaker selection is associated with a larger range of  $h$  values for which the conditional fixation  
323 time is greater than the neutral value.

324 A critical value of the dominance coefficient for a given  $\gamma$ ,  $h_{cf}(\gamma)$ , can be defined, which is  
325 the value of  $h$  at which the mean fixation time is equal to the neutral value. A similar quantity,  
326  $h_{cl}(\gamma)$ , can be defined for the mean time to loss. As is discussed in more detail in the section  
327 *Relevance to associative overdominance and background selection*, these quantities provide a  
328 useful link between the present approach and that of Zhao and Charlesworth (2016), who examined  
329 the conditions for AOD versus BGS for the case of a large population that is initially in stochastic  
330 equilibrium under mutation, drift and selection, and then suffers a permanent reduction in  
331 population size. As a measure of the magnitude of genetic drift, they used the asymptotic rate at  
332 which variability at a neutral site linked to a site under selection decreases after the reduction in  $N$ ,  
333 and determined whether selection increased or reduced the rate of loss of variability.

334 Approximations for the critical dominance coefficients that correspond to the boundary  
335 between an increased and a decreased mean fixation or loss time can be obtained by setting the sum  
336 of the terms involving  $\gamma$  and  $\gamma^2$  to zero in Equations (2) and (3), and solving the resulting quadratic  
337 equations in  $h$ . For  $h_{cf}(\gamma)$ , the further approximation of replacing 59/300 with 1/5 is used.

338 After some algebra, the following expressions are obtained:

339

340 
$$h_{cf}(\gamma) \approx \frac{1}{2}\gamma^{-1}\{\gamma - 10 + 10\sqrt{1 + 0.05\gamma^2}\} \quad (8a)$$

341 
$$h_{cl}(\gamma) \approx (0.264\gamma)^{-1}\{0.282\gamma - 1 + \sqrt{1 - 0.3\gamma + 0.08550\gamma^2}\} \quad (8b)$$

342

343 As  $\gamma$  approaches zero, consideration of the leading terms in  $\gamma$  in the radicals in these  
344 equations shows that the critical dominance coefficient  $\approx 0.5 + 0.125\gamma$  in both cases, so that slightly  
345 recessive mutations ( $\gamma < 0$ ) or dominant mutations ( $\gamma > 0$ ) result in an increase in mean fixation and  
346 loss times when selection is very weak. For small  $\gamma$ , which is the main region of interest as far as  
347 AOD is concerned, the critical dominance coefficients are nearly linear in  $\gamma$  (Figure 4).

348 The blue curves in Figure 4 show the critical dominance coefficients for the operation of  
349 AOD, given by the solution of the approximate cubic Equation (18) of Zhao and Charlesworth  
350 (2016). For favorable mutations, this expression breaks down for  $\gamma > 1.26$ , but performs well for  
351 deleterious mutations over the entire range displayed. If the cubic equation is approximated by  
352 ignoring terms in  $\gamma^2$ , the critical dominance coefficient for the operation of AOD is  $0.5 + 0.125\gamma$ , the  
353 same as for  $h_{cf}$  and  $h_{ct}$ . This suggests that the two approaches are related to each other, although the  
354 three different functions describing  $h_c$  do not agree precisely.

355

### 356 **Effects of weak selection on variability at linked neutral sites**

357 Intuitively, one would expect the longer mean fixation times associated with weak selection and  $\gamma < 0$   
358 to produce a higher level of mean pairwise diversity ( $\pi$ ) at a linked neutral site than when a  
359 neutral mutation has become fixed. This was shown to be the case by Mafessoni and Lachmann  
360 (2015) and Johri *et al.* (2021), using computer simulations (similar, but smaller, effects would be  
361 expected from losses of new mutations; these were not, however, examined in these papers). Note,  
362 however, that the fixation of a neutral mutation produces an approximately 42% reduction in  $\pi$  at  
363 completely linked sites (Tajima 1990), so that all these cases are still associated with reduced rather  
364 than increased diversity. This is because  $\pi$  is measured at a single point in time (when a new  
365 mutation has been fixed), rather than using an estimate of the mean of  $\pi$  over a long time period at a  
366 focal neutral site that is subject to a succession of evolutionary events at a linked site – if this site is  
367 neutral, the mean  $\pi$  at the focal site cannot be affected by these events. An approximate method for  
368 calculating  $\pi$  at the end of a fixation event was used by Johri *et al.* (2021), based on the selective  
369 sweep equations of Charlesworth (2020b); this procedure is, however, unsatisfactory, since the  
370 sweep equations are inaccurate at small  $|\gamma|$  values.

371 A first step towards obtaining an estimate of the long term mean value of  $\pi$  is to determine  
372 the pattern of variability at a focal neutral site over the course of fixation (or loss) of a linked  
373 mutation ( $A_2$ ) introduced into a population initially fixed for the alternative allele ( $A_1$ ). This was

374 done here by applying the simulation procedure of Tajima (1990), as described in the Material and  
375 Methods section and in Johri *et al.* (2021). The left-hand panel in Figure 5 shows the results for  
376 fixations of a favorable mutation with dominance coefficient  $h = 0.9$  and a range of values of the  
377 scaled selection coefficient,  $\gamma$  in a population size of 50, and with complete linkage between the  
378 neutral and selected sites. All diversity statistics are measured relative to  $\theta = 4N_e\mu$ , the equilibrium  
379 value in the absence of selection. It will be seen that the mean relative  $\pi$  over all genotypes taken  
380 over a fixation event ( $\pi_w$ ) exceeds one for sufficiently small  $\gamma$  values, even for the neutral case of  $\gamma$   
381  $= 0$ , whereas the relative  $\pi$  at the time of fixation or loss is always  $< 1$ . The reason for the excess in  
382  $\pi_w$  over neutral expectation is that the slowness of the fixation process (whose expected value is of  
383 the order of  $4N_e$  generations with weak selection) allows  $A_1$  and  $A_2$  haplotypes to diverge in  
384 sequence over the course of the fixation of  $A_2$ , because their mean coalescent times in the absence  
385 of recombination are much greater than the standard neutral value of  $4N_e$  generations (Kimura and  
386 Ohta 1969). Comparable results are seen for losses of new mutations, but with much smaller effects  
387 due to the shorter expected duration of loss events, which is close to  $2 \ln(N_H)$  generations with weak  
388 selection (Figure S4).

389 These results yield the seemingly paradoxical conclusion that fixation and loss events can be  
390 associated with a net increase in mean  $\pi$  at linked neutral sites during the course of fixation or loss,  
391 even when they involve neutral mutations. The paradox with respect to neutral mutations comes  
392 from the fact that one type of conditional event has been replaced by another: we are conditioning  
393 on observing a fixation or loss event that is in progress, and the increasing divergence between  
394 haplotypes carrying the ancestral and mutant alleles influences the net effect of the fixation or loss  
395 event on variability at the neutral site, as discussed in more detail below.

396 The following approximate approach avoids such conditioning. As was done by  
397 Charlesworth (2020b) for the case of sweeps of strongly selected mutations, ergodicity is assumed:  
398 the probability of a given value of  $\pi$  resulting from the hitchhiking effects of the selected site is  
399 proportional to the amount of time that the process spends at that value of  $\pi$ , analogous to the use of  
400 the sojourn time density for determining the frequency spectrum at a single locus (Ewens 2004  
401 pp.24-25).

402 A core assumption is that the rates of fixation and loss events are sufficiently low that the  
403 intervals between successive events allow a complete recovery of diversity. Once again, diversities  
404 are measured relative to the value in the absence of selection, and the deviation of the relative  
405 diversity value from one is denoted by  $\Delta\pi$ . If the mean value of  $\Delta\pi$  immediately after a given  
406 fixation or loss event is denoted by  $\Delta\pi_0$ , and the value of  $\Delta\pi$  at time  $t$  after such an event is  $\Delta\pi_t$ , we

407 have  $\Delta\pi_t \approx \Delta\pi_0 \exp(-t)$ , where  $t$  is in units of  $2N_e$  generations (Malécot 1969, p.40; Wiehe and  
408 Stephan 1993, Equation 6a). The sum of the values of  $\Delta\pi_t$  over subsequent generations, relative to  
409  $2N_e$ , can thus be approximated by:

410

$$411 \quad \Delta\pi_0 \int_0^{\infty} \exp(-t) dt = \Delta\pi_0 \quad (9)$$

412

413 We also need to consider the contribution from the mean diversity over the course of each  
414 fixation (loss) event, which is given by the expectation of the product of the duration of an event,  
415  $T_e$ , and the associated mean value per generation of  $\Delta\pi$  over the course of the event,  $\Delta\pi_w$ , *i.e.*, by  
416  $E\{T_e\Delta\pi_w\}$ . If  $T_e$  is measured in units of coalescent time, and we use the sum of the  $\Delta\pi$  values  
417 relative to  $2N_e$  over a long period of time (or over many independent pieces of genome that are all  
418 subject to the same evolutionary process), the mean sum of the deviation from 1 of the relative  
419 diversity between successive fixation (loss) events is given by:

420

$$421 \quad \Delta\pi_S = \Delta\pi_0 + E\{T_e\Delta\pi_w\} \quad (10)$$

422

423 To calculate the change in mean relative diversity due to a succession of evolutionary  
424 events, we would of course need to know the total length of time involved, requiring a calculation  
425 of the expected number of occurrences of fixation (loss) events and the expected times between  
426 them (see the next section). Use of Equation (10) avoids having to make a detailed model of these  
427 events, and provides an index of the expected magnitude and sign of the effects on neutral diversity  
428 of fixations (losses) at a linked site.  $\Delta\pi_S$  can thus be (loosely) referred to as the mean change in  
429 diversity associated with a series of fixation or loss events.

430

431 It should be noted that the assumption of an indefinitely large amount of time for recovery  
432 of diversity between fixation or loss events implies that the contribution of  $\Delta\pi_0$  relative to  $E\{T_e\Delta\pi_w\}$   
433 is overestimated compared with a realistic evolutionary model, so that any increases in diversity  
434 with weak selection when  $\gamma b < 0$  will be underestimated by this approach when  $\Delta\pi_0 < 0$  and  
435  $E\{T_e\Delta\pi_w\} > 0$ .

436

437 Numerical values of the quantities involved can be obtained from the simulations of a  
438 neutral sites linked to a locus subject to selection, using the algorithm of Tajima (1990), as  
439 described in the Material and Methods. The relevant statistics are shown in the left-hand panel of  
438 Figure 5 for the case of the fixation of a partially dominant, favorable mutation ( $h = 0.9$ ) in a  
439 population with  $N = 50$ . Using Equation (10),  $\Delta\pi_S$  for recurrent fixations is shown in the right-hand

440 panel of Figure 5, for  $N = 50$  and  $N = 500$ . Here, the mean of  $T_e\Delta\pi_w$  over many replicate simulations  
441 is used as an estimate of the expectation of  $T_e\Delta\pi_w$ .

442 It can be seen that fixations of highly dominant, favorable mutations cause an increase in  
443 diversity when  $\gamma$  is sufficiently small, but diversity is reduced when  $\gamma$  is somewhat greater than 2;  
444 the value of  $\gamma$  at the point of return to a reduction in  $\pi$  is smaller with the larger value of  $N$ . As  
445 expected from the properties of the mean fixation time described above, a similar pattern (within the  
446 limits of statistical error) is observed for fixations of deleterious mutations with  $h = 0.1$  and the  
447 same absolute value of  $\gamma$  (Figure S4). Figures 6 and S5 show comparable results for losses of both  
448 favorable and deleterious mutations; in this case, the patterns are noticeably different for the two  
449 types of mutations, and are much more strongly affected by the population size, as expected from  
450 the corresponding effects on mean loss times described in the previous section. Tables S1-S8 show  
451 the detailed statistics for the simulations on which these figures are based, and Table S9 shows  
452 summary diversity statistics for fixation and loss events for a range of dominance coefficients, and  
453 two different strengths of positive and negative selection.

454 The results allow questions to be asked about the nature of the major determinant of the  
455 effect of selection on neutral diversity at a linked site. Intuitively, it would seem likely that the  
456 mean conditional times to fixation,  $t^*$ , and loss,  $t^{**}$ , must play a major role. However, the answer  
457 depends on what aspect of diversity is being explored. A detailed discussion of results relating to  
458 this question is given in section 2 of Supplementary File 1, section 1. These results show that, for a  
459 given value of  $\gamma$ , both sojourn times are nearly linearly related to the diversity statistics, but the sign  
460 and magnitude of  $\gamma$  influence the values of the diversity statistics for the same value of  $t^*$  or  $t^{**}$ .  
461 There is a close correspondence between the values of  $t^*$  and  $t^{**}$  that are generated by the  
462 simulations with  $\gamma = 0$  and the thresholds at which  $\Delta\pi_S \geq 0$ , within the limits of sampling error  
463 (Figures S6 and S9).

464 The results can be interpreted as follows. The mean neutral diversity of haplotypes carrying  
465 the selectively favorable  $A_2$  variant increases with the duration of a fixation event, because these  
466 haplotypes spend longer in the population before reaching fixation and hence have a longer  
467 coalescence time. The divergence between  $A_1$  and  $A_2$  haplotypes also increases with  $t^*$ , since a  
468 longer time is available for them to diverge. The changes in the diversity of  $A_1$  haplotypes are more  
469 minor. The net result is that the net mean diversity over the course of the event ( $\Delta\pi_w$ ) increases with  
470  $t^*$ , as can be seen in Figure S7, so that its product with  $t^*$ , which appears in the equation for  $\Delta\pi_S$   
471 (Equation 10) also increases with  $t^*$ . This effect is reinforced by the decline in the reduction of



472 diversity at the time of fixation of  $A_2$ ,  $-\Delta\pi_0$ , as  $t^*$  increases (Figure S8), reflecting a greater  
473 coalescence time for  $A_2$  when its sojourn time is longer.

474         These considerations apply to both positive and negative selection. However, with positive  
475 selection,  $A_2$  spends more of its time at high frequencies than at low frequencies before becoming  
476 fixed, whereas the reverse is true with negative selection, as can be seen in the plots of the sojourn  
477 time densities relative to the neutral values that are shown in Figure 8 (note that  $t^*(x)$  is independent  
478 of  $x$  in the absence of selection). This means that, for the same  $|\gamma|$  value, haplotypes carrying  $A_1$   
479 have a longer coalescence time with negative than with positive selection; because these haplotypes  
480 start with the equilibrium neutral diversity value  $\theta$ , they contribute disproportionately to  $\Delta\pi_w$ . This  
481 effect is especially clear for the larger values of  $|\gamma|$ ; for example, with  $|\gamma| = 5$ , the mean diversity of  
482  $A_1$  haplotypes is  $0.657 \pm 0.001$  for  $\gamma = -5$ , and  $0.608 \pm 0.001$  for  $\gamma = 5$ .

483         Similar patterns are seen with losses of mutations. This is perhaps less surprising, since  $t^{**}$   
484 for a given  $|\gamma|$  value is greater for deleterious mutations than for favorable mutations when  $h$  for the  
485 former is the same as  $1 - h$  for the latter, i.e., the dominance coefficients are complementary (Figure  
486 3).

487

#### 488 **Relevance to associative overdominance and background selection**

489 As mentioned in the Introduction, the relevance of these results to associative overdominance  
490 (AOD) arises from the fact that, if selection is sufficiently weak in relation to genetic drift, a  
491 biallelic locus subject to selection and reversible mutations will experience a constant flux of  
492 mutations from the states of fixation for  $A_1$  to fixation for  $A_2$  and vice-versa, as in the Li-Bulmer  
493 model of codon usage bias (Li 1987; Bulmer 1991; McVean and Charlesworth 1999). Here,  $A_1$  is  
494 now used to denote the selectively favorable allele at a given site, and  $A_2$  its deleterious alternative,  
495 rather than ancestral and mutant alleles, respectively.

496         For the case of an autosomal locus, the relative fitnesses of the three genotypes  $A_1A_1$ ,  $A_1A_2$   
497 and  $A_2A_2$  are  $1$ ,  $1 - hs$  and  $1 - s$ , respectively ( $s \geq 0$ ); with weak selection, this is equivalent to  
498 representing these fitnesses as  $1 + s$ ,  $1 + (1 - h)s$  and  $1$ . Thus, if the deleterious effects of  $A_2$  are  
499 recessive or partially recessive ( $0 \leq h < 0.5$ ) and  $\gamma = 2N_e s$  is sufficiently small, the entry of an  $A_2$   
500 mutation into a population temporarily fixed for  $A_1$  will be associated with a longer net sojourn time  
501 in the population than that for a neutral mutation. The same applies to the entry of a favorable  $A_1$   
502 mutation into a population temporarily fixed for  $A_2$ .

503         The results in the previous section strongly suggest that, under these conditions, diversity at  
504 closely linked neutral sites will be enhanced when a stationary state with respect to mutation,



505 selection and drift is reached. The effect of the constant flux of mutations at a selected site on the  
506 expected level of neutral diversity ( $\pi$ ) at the linked neutral site can be determined with the use of the  
507 ergodic assumption. This allows the application of the results of the simulations described above  
508 that used this approach, employing the infinite sites assumption that mutations are sufficiently  
509 infrequent that new mutations occur only at sites that are fixed for either  $A_1$  or  $A_2$ , which was  
510 applied to the theory of codon usage by Bulmer (1991) and McVean and Charlesworth (1999).  
511 Table 1 shows the variables that are used in this procedure. As in the previous section, diversity is  
512 measured relative to the purely neutral equilibrium value  $\theta = 4N_e\mu$ , and its deviation from one at  
513 given point in time is denoted by  $\Delta\pi$ .

514 Consider a site that has just become fixed for  $A_1$ . Under the above assumptions, the  
515 distribution of times until an  $A_2$  mutation arises and becomes fixed is exponential, with parameter  
516  $\lambda_{11}$ . If a time  $t$  is drawn from this distribution, the expected number of  $A_2$  mutations that arise and  
517 become lost during an interval of length  $t$  is  $\lambda_{10}t$ , where  $\lambda_{10} \gg \lambda_{11}$  from the formulae in Table 1.  
518 Integrating over the distribution of  $t$ , the expected number of losses of  $A_2$  mutations before  $A_2$   
519 becomes fixed is found to be approximately equal to  $\lambda_{10}/\lambda_{11} = P_{10}/P_{11}$ . If the times between each  
520 successive event are  $\gg 1$ , diversity completely recovers between loss events, and between the  
521 initial fixation and first loss event (it is shown below that this assumption can be relaxed). Applying  
522 Equation (10) from the previous section, and using the notation in Table 1, the expected sum  
523 (relative to  $2N_e$ ) of  $\Delta\pi$  values at the neutral site over the interval between the successive fixation  
524 events  $A_2$  to  $A_1$  and  $A_1$  to  $A_2$  is given by:

525

$$526 \quad \Delta\pi_1 \approx \Delta\pi_{1f} + (\lambda_{10}/\lambda_{11}) \Delta\pi_{10s} \quad (11a)$$

527

528 A similar argument applies to the interval succeeding the fixation of the  $A_2$  mutation and  
529 another fixation of an  $A_1$  mutation, substituting 2 for 1 in the first subscripts for the  $P$ s and  $\lambda$ s in  
530 Table 1 ( $\lambda_{20} \gg \lambda_{21}$  is assumed), giving:

531

$$532 \quad \Delta\pi_2 \approx \Delta\pi_{2f} + (\lambda_{20}/\lambda_{21}) \Delta\pi_{20s} \quad (11b)$$

533

534 The expectation of the sum of  $\Delta\pi$  values over an entire cycle between successive fixations  
535 of  $A_1$  mutations is simply  $\Delta\pi_T = \Delta\pi_1 + \Delta\pi_2$ . We can thus estimate the expected value of  $\Delta\pi_T$  per

536 generation,  $\Delta\pi_e$ , by dividing  $\Delta\pi_T$  by the expected time between successive fixations of  $A_1$  (in units  
537 of  $2N_e$  generations),  $T_s = (\lambda_{11}^{-1} + \lambda_{21}^{-1})$ :

538

$$539 \quad \Delta\pi_e = \frac{\Delta\pi_1 + \Delta\pi_2}{T_s} \quad (11c)$$

540

541 It is useful to note that the expression for  $T_s$  is consistent with the existence of a stationary  
542 state for the proportion of sites fixed for  $A_1$  versus  $A_2$ , using the infinite sites assumption. If these  
543 proportions are denoted by  $X$  and  $1 - X$ , respectively, stationarity exists if  $\lambda_{11}X = \lambda_{21}(1 - X)$ , i.e.,  $X =$   
544  $\lambda_{21}/(\lambda_{11} + \lambda_{21})$  (Bulmer 1991; McVean and Charlesworth 1999). At stationarity, the proportion of  
545 sites that are fixed for  $A_1$  is proportional to the expected time a site spend in that state, so that  $X =$   
546  $\lambda_{11}^{-1}/(\lambda_{11}^{-1} + \lambda_{21}^{-1}) = \lambda_{21}/(\lambda_{11} + \lambda_{21})$ .

547 All the quantities needed for determining the value of  $\Delta\pi_e$  in Equation (11c), other than the  
548 mutational parameters at the selected site,  $\theta_s$  and  $\kappa_s$  can be obtained from the integral formulae for  
549 the fixation probabilities, together with the simulation methods described in the previous section.  
550 The mutational parameters serve only to determine the magnitude of  $\Delta\pi_e$ , and have no influence on  
551 its sign, provided that the assumptions concerning the times to recovery after fixation and loss  
552 events and the relative values of  $\lambda_{i0}$  and  $\lambda_{i1}$  are met. The general equations above are valid regardless  
553 of the frequency of recombination; the values of the  $\Delta\pi$  variables that appear in these expressions  
554 will, of course, be affected by recombination.

555 Figure 7 shows an example of estimates of  $\Delta\pi_e$  for the case of a neutral locus that is  
556 completely linked to a selected locus with equal mutation rates in each direction between  
557 deleterious and favorable alleles ( $\kappa = 1$ ), as a function of the scaled selection coefficient,  $\gamma$ . The  
558 deleterious allele ( $A_2$ ) has dominance coefficient  $h = 0.1$ , such that the relative fitnesses of  
559 heterozygotes and homozygotes for this allele are  $1 - 0.1s$  and  $1 - s$ , respectively. As expected from  
560 the previous results, the enhancement of diversity is maximal (approximately 0.008 with  $N = 500$ )  
561 when  $\gamma = 1.5$ . The fact that  $\Delta\pi_e$  is significantly negative for  $\gamma = 0$  suggests that, as noted above, the  
562 assumption of a long recovery period between successive losses or fixations at the selected locus  
563 results in an underestimation of  $\Delta\pi_e$  for small  $\gamma$ .

564 In the example in the figure, the scaled mutation rate at the selected locus was 0.01 for both  
565 population sizes, corresponding to an absolute mutation rate of  $5 \times 10^{-5}$  with  $N = 50$  and  $5 \times 10^{-6}$   
566 with  $N = 500$ ; the results are not very sensitive to the absolute value of  $N$  for the same set of scaled  
567 parameters, so that the approximate values for an arbitrary  $\theta_s$  can be obtained by multiplying the

568 results in the figure by  $100\theta_s$ . In a population of size 10,000, the mutation rate would be  $1.25 \times 10^{-7}$ ,  
569 corresponding to a non-recombining region with 25 basepairs under selection with mutation rate is  
570  $0.5 \times 10^{-8}$  per basepair, which is approximately the same as the estimate for *Drosophila*  
571 *melanogaster* (Assaf *et al.* 2017).

572 A check on the validity of this approach is provided by the case when  $\gamma$  is so large that the  
573 rate of fixation of deleterious mutations is negligible. This means that only the state when the  
574 population is fixed for the favorable allele  $A_1$  needs to be considered. There is then a constant input  
575 of new mutations to  $A_2$  alleles, which are successively lost from the population with a probability  
576 close to 1. This situation corresponds to the standard model of background selection (BGS), under  
577 which stochastic effects at the loci under selection are assumed to be negligible (Charlesworth *et al.*  
578 1993). In this case, however, the assumption of a complete recovery of diversity at the neutral locus  
579 after each loss event is likely to be violated, as the large population size means that there is a high  
580 rate of input of new deleterious mutations that are then rapidly lost from the population, especially  
581 if we are dealing with a non-recombining region with numerous genes subject to purifying  
582 selection.

583 This problem is examined in the second part of the Appendix, where it is shown that the  
584 results obtained with the assumption of complete recovery should still provide a good  
585 approximation in this case. The deviation of mean relative diversity from one can be predicted from  
586 the sum of the  $\Delta\pi$  values over the period covering the loss of an  $A_2$  allele and the appearance of a  
587 new mutation to  $A_2$ , as given by Equation (10), divided by the expected time between successive  
588 losses of deleterious mutations (equivalent to multiplication by  $\lambda_{10}$ ), as can be seen from Equation  
589 (A12). This prediction can be compared to the standard BGS formula for autosomal loci in a  
590 randomly mating population, which assumes that allele frequencies subject to selection are  
591 unaffected by drift, i.e.,  $\gamma \gg 1$ . In this case, the reduction in diversity relative to neutral expectation  
592 at a neutral site completely linked to a selected locus or group of loci is approximately equal to  $u/hs$   
593 provided that  $u/hs \ll 1$ , where  $u$  is the net rate of mutation to deleterious alleles (Charlesworth *et*  
594 *al.* 1993). This can be equated to  $\Delta\pi_e$  for the same values of  $u$ ,  $h$  and  $s$  when applying Equation  
595 (11c) to the simulations used here. To model large  $\gamma$  values while retaining the assumption of small  
596  $s$ , it is necessary to use simulations with a large population size ( $N = 500$ ). To generate these  
597 numbers, the scaled rate of mutation to deleterious mutations,  $\theta_s$ , was arbitrarily set to 1; the values  
598 for an arbitrary deleterious mutation rate of  $u$  can be found by multiplying these values by  $4Nu$ .  
599 Some examples are shown in Table 2; it can be seen that the predictions from the present approach  
600 converge on the values from the large population size formula as  $h\gamma$  increases.

601 Stochastic fluctuations in the frequencies of alleles at selected loci are known to reduce the  
602 effect of BGS on diversity (Charlesworth *et al.* 1993). Table 1 of Charlesworth *et al.* (1993) gives  
603 simulation results for a range of  $\gamma$  values for the case of a non-recombining region with a deleterious  
604 mutation rate of  $u = 0.005$ ,  $s = 0.1$  and  $h = 0.2$ , so that  $u/hs = 0.25$ . The ratio of the negative of the  
605 natural logarithm of a simulated value of  $\pi/\theta$  to 0.25 provides a measure of the extent of the  
606 deviation from the deterministic prediction. These measures (with their standard errors) were as  
607 follows:  $0.696 \pm 0.024$  ( $\gamma = 20$ ),  $0.892 \pm 0.035$  ( $\gamma = 40$ ),  $0.828 \pm 0.054$  ( $\gamma = 80$ ) and  $1.056 \pm 0.049$   
608 ( $\gamma = 180$ ). The corresponding ratios from the present method for these parameter sets were  
609  $0.510 \pm 0.015$ ,  $0.858 \pm 0.020$ ,  $0.992 \pm 0.020$  and  $1.124 \pm 0.016$ , respectively. In view of the  
610 approximations needed to obtain these results, there is reasonably good agreement with the exact  
611 simulation results.

612 The argument concerning the effect of the times between events presented in the Appendix  
613 can be extended to the case when there is a continual flux between  $A_1$  and  $A_2$  alleles, as in the case  
614 of the model of AOD discussed above. Here, the probabilities of fixation of both variants are of the  
615 order of  $1/N_H$ , whereas the probabilities of loss are of the order of one. The expected numbers of  
616 loss events between successive fixations are thus of order  $N_H$  for both types of event. Provided that  
617  $N_H$  is not too small, the argument leading to Equation (A.12) implies that the net effect on diversity  
618 is similar to the value when there is a complete recovery between loss events, so that Equation (11c)  
619 should provide a good approximation to the effects of successive losses, but there will still be an  
620 inaccuracy associated with the recovery period following a fixation event.

621

## 622 **Discussion**

623

624 The analytical and simulation results described here shed light on the effects of the fixations and  
625 losses of weakly selected or neutral mutations on levels of genetic diversity at linked neutral sites,  
626 first studied by Tajima (1990), and which have recently received renewed attention in the  
627 population genetics literature (Mafessoni and Lachmann 2017; Johri *et al.* 2021; Kaushik and Jain  
628 2021; Moinet *et al.* 2021). As described in the previous two sections, these effects can largely be  
629 understood in terms of the effects of the selection parameters on the times to fixation or loss,  
630 conditioned on fixation or loss, with some slight complications.

631

## 632 **Conditional fixation and loss times with weak selection**

633 One might expect selection on favorable mutations to reduce their mean time to fixation relative to  
634 neutrality, and selection against deleterious mutations to have the opposite effect, with the converse  
635 applying to losses of mutations. As described above, this is not necessarily the case. Mafessoni and  
636 Lachmann (2015) used numerical integration of the relevant diffusion equation formulae for  
637 autosomal mutations with random mating to show that the mean fixation times (conditioned on  
638 fixation) of weakly selected dominant or partially dominant ( $h > 1/2$ ) mutations, as well as of weakly  
639 selected, recessive or partially recessive ( $h < 1/2$ ) deleterious mutations, can be larger than the  
640 corresponding neutral values. They also showed that, under similar conditions, the mean conditional  
641 times to loss of new mutations are larger than the neutral values. For sufficiently large values of the  
642 magnitude of the scaled selection coefficient,  $|\gamma| = 2N_e|s|$ , however, fixation and loss times are  
643 always lower than the neutral values when there is directional selection ( $0 \leq h \leq 1$ ). The  
644 approximations derived here (Equations 2 and 3), which are accurate with respect to second-order  
645 terms in  $\gamma$ , confirm these findings (see also Kaushik and Jain 2021, Equation 9). They provide a  
646 reasonably good fit to the numerical integration and simulation results for  $|\gamma|$  values of the order of  
647 2 or less, provided that the population size is sufficiently large (Figures 1 and 2).

648

#### 649 **Effects of weak selection on neutral diversity at linked sites**

650 Mafessoni and Lachmann (2015) also showed that fixations of partially recessive favorable or  
651 partially dominant deleterious mutations can increase the mean level of diversity ( $\pi$ ) at a linked  
652 neutral site, compared with the corresponding value for fixations of neutral mutations, if this is  
653 measured at the time of fixation. The conditions for such an increase are similar to those for an  
654 increased time to fixation (see also Johri *et al.* [2021] and Kaushik and Jain [2021]). The simulation  
655 results described here confirm this finding, and give similar results for losses of deleterious  
656 mutations (Figures 5, S4 and S5). However, the diversity levels at the times of fixation or loss are  
657 always lower than the mean equilibrium neutral diversity,  $\theta = 4N_e\mu$ , even if these events involve  
658 purely neutral mutations, as was first described by Tajima (1990). As was explained in the section  
659 *Effects of weak selection on variability at linked neutral sites*, this effect is a consequence of  
660 conditioning on an unusually short coalescent time at the neutral site linked to the site under  
661 observation, and would not be expected to occur if we observe the mean diversity at this site over a  
662 long time period that includes multiple fixation or loss events. The question of whether diversity  
663 can be increased above  $\theta$  by weak selection under appropriate conditions is thus not fully answered  
664 by these results.

665           A simple approximate method for evaluating the effects of successive fixations or losses at a  
666 site linked to focal neutral site was described above (Equation 10). This combines the sum of the  
667 diversities at the focal site over the generations while a fixation or loss event is in progress with the  
668 sum of the diversities over the generations that intervene until the next such event, during which  
669 diversity recovers towards the neutral equilibrium value. As shown in Figures 5, S4 and S5, the  
670 mean diversity taken over all generations during a fixation or loss event can be increased over the  
671 neutral value when  $|\lambda|$  is sufficiently small, and  $h < 1/2$  for deleterious mutations or  $> 1/2$  for favorable  
672 ones, partly due to mutational divergence between the haplotypes carrying the two different alleles  
673 at the site under selection. Under suitable conditions (a sufficiently long duration of the fixation or  
674 loss event), this effect can outweigh the reduction in diversity at the end of the fixation or loss  
675 event, resulting in a net increase in mean neutral diversity when taken over the entire period.

676           These considerations yield the seemingly paradoxical result that neutral diversity can be  
677 enhanced by fixations or losses of weakly selected favorable or deleterious mutations, in contrast to  
678 the usual assumption that diversity is reduced by fixations of favorable mutations (selective sweeps)  
679 or losses of deleterious mutations (background selection). It has, however, long been known that  
680 neutral diversity can in principle be increased by selection against deleterious recessive or partially  
681 recessive mutations at closely linked sites – the process of associative overdominance or AOD  
682 (Frydenberg 1963; Ohta 1971; Latter 1998; Pamilo and Palsson 1998; Palsson and Pamilo 1999;  
683 Wang and Hill 1999; Becher et al. 2020; Gilbert et al. 2020; Waller 2021). A correct analytical  
684 treatment of this process for the simplest case of a single selected locus and a linked neutral locus  
685 has, however, only recently been provided (Zhao and Charlesworth 2016). As shown in Figure 4,  
686 the critical dominance coefficient for the operation of AOD versus background selection (BGS) as a  
687 function of  $|\lambda|$  has similar, but not identical, properties to the conditions for increases over the  
688 neutral value of the mean conditional fixation and loss times of new deleterious or favorable  
689 mutations.

690           The section *Relevance to associative overdominance and background selection* describes  
691 how to relate the simulation results for the effects of selection on the diversity statistics at a linked  
692 neutral locus, when there is a continual flux of mutations between sites fixed for deleterious and  
693 favorable mutations. Under this scenario, the net mean deviation from one of  $\pi/\theta$  is given by  $\Delta\pi_e$  in  
694 Equation (11c). Fixations and losses contribute approximately equal amounts to  $\Delta\pi_e$ ; although the  
695 effects on diversity of losses are much smaller than those of fixations, this is offset by the much  
696 higher frequencies of loss events.

697           The results described here provide a new perspective on the relation between AOD and  
698 BGS. If one imagines a locus subject to reversible mutation between a wild-type allele ( $A_1$ ) and a  
699 deleterious allele ( $A_2$ ), the standard model of BGS corresponds to the situation when selection  
700 against  $A_2$  is so strong ( $|\gamma| \gg 1$ ) that there is effectively no possibility of fixations of reverse  
701 mutations to  $A_1$ , and the system can be treated as though it is at equilibrium under mutation and  
702 selection, as in the standard formulae used to describe the effect of BGS on neutral diversity  
703 (Charlesworth, et al. 1993; Hudson and Kaplan 1995; Nordborg, et al. 1996). In reality, the  
704 population size is finite, so mutations from  $A_1$  to  $A_2$  are constantly occurring and being quickly lost  
705 from the population, with a probability close to one when  $|\gamma| \gg 1$ . As shown in Table 2, the  
706 application of the approach described here to this situation closely approximates the properties of  
707 BGS when finite population size is modeled by exact simulations.

708           If  $|\gamma|$  is sufficiently small, however, the effects of genetic drift and reversible mutation  
709 between  $A_1$  and  $A_2$  need to be considered jointly, as in the Li-Bulmer model of selection on codon  
710 usage (Li 1987; Bulmer 1991; McVean and Charlesworth 1999). With  $|\gamma| \leq 2$  or so and  $h$  for  
711 deleterious mutations less than  $\frac{1}{2}$ , the results enshrined in Equations (11) show that diversity at  
712 linked neutral sites can be increased over neutral expectation when the population is at statistical  
713 equilibrium under drift, mutation and selection for sites under selection. These findings complement  
714 the results of the analysis of AOD by Zhao and Charlesworth (2016), who examined the rate of loss  
715 of neutral variability in a population that was initially at statistical equilibrium, and then placed into  
716 an environment with a relatively small  $N_e$ . As noted already, the conditions on the dominance  
717 coefficient as a function of  $|\gamma|$  that allow an enhancement of variability are similar for the two  
718 approaches. The framework described here is more appropriate than that of Zhao and Charlesworth  
719 (2016) for populations maintained for a long time at low effective population sizes, as is the case in  
720 some laboratory experiments that have yielded evidence for AOD (Latter 1998), and for low  
721 recombining genomic regions in large populations, where recent work has also suggested the  
722 operation of AOD (Becher *et al.* 2020; Gilbert *et al.* 2020).

723

#### 724 **Interpreting the effects of selection on the conditional sojourn times, $t^*$ and $t^{**}$**

725 Here, intuitive interpretations are presented of the conditions for increases in the mean conditional  
726 times to fixation ( $t^*$ ) and loss ( $t^{**}$ ) over their neutral expectation. A more rigorous approach to this  
727 question is given in Supplementary File S1, section 3. One important point to note is that Equations  
728 (2) and (3) show that the first-order terms in  $\gamma u$  in the expressions for  $t^*$  and  $t^{**}$  are zero when  $b = 0$   
729 ( $h = \frac{1}{2}$  for autosomal mutations), so that the conditional sojourn times are then approximately the



730 same as with neutrality when selection is very weak. This finding suggests that the first-order  
731 effects of selection that depend on the term in  $\gamma a$  in Equation (1) are absorbed into the probabilities  
732 of fixation and loss, so that the conditional sojourn times are controlled by  $\gamma b$  alone when selection  
733 is very weak. Another relevant point is that the relative effectiveness of selection versus drift can be  
734 quantified by dividing Equation (1) by  $x(1-x)$ , which gives the ratio of the selective change in  
735 allele frequency per generation to the sampling variance under drift,  $x(1-x)/2N_e$ . This ratio is  
736 denoted here by  $f(x) = \gamma(a + bx)$ . If  $\gamma b < 0$ , the relative effectiveness of selection in causing a  
737 movement of  $x$  away from zero, as measured by  $f(x)$ , is reduced, compared with the quasi-neutral  
738 case with  $\gamma b = 0$ , and decreases as  $x$  increases.

739         The condition for weak selection to cause an increase in  $t^*$  over neutrality is then relatively  
740 easy to interpret (see Mafessoni and Lachmann (2015) for a different viewpoint). If  $\gamma > 0$  and  $b < 0$   
741 ( $h > 1/2$  for an autosomal mutation),  $x$  tends to be decreased by selection compared with quasi-  
742 neutrality, especially at larger values of  $x$ , so that the net time to reach fixation is increased by  
743 selection, and the times spent at larger values of  $x$  are increased relative to the neutral case. If  $\gamma < 0$   
744 and  $b > 0$  ( $h < 1/2$  for an autosomal mutation), there is a stronger tendency for  $x$  to move towards  
745 zero than under quasi-neutrality; because we are conditioning on fixation of  $A_2$ , this causes the  
746 sojourn time to be increased over neutrality. The pull towards lower values of  $x$  is weaker for small  
747  $x$ , so that the time spent at low values of  $x$  is increased relative to the neutral case. These effects on  
748 the sojourn time densities at different frequencies are illustrated in the lower panels of Figure 8.

749         It is less easy to interpret the properties of  $t^{**}$ , because the argument used for  $t^*$  would at  
750 first sight suggest a reduction rather than an increase in  $t^{**}$  when  $\gamma b < 0$ . The most plausible  
751 interpretation is that losses of new mutations are largely caused by drift, and take place rapidly as  
752 long as  $x$  remains close to zero. However, the time for an  $A_2$  mutation to reach a relatively high  
753 frequency is increased by weak selection when  $\gamma b < 0$ . It is then relatively immune to loss, and  
754 hence spends longer segregating in the population. This interpretation is consistent with the fact that  
755 the sojourn time densities relative to the neutral values are increasing functions of  $x$  for both  
756 favorable and deleterious mutations, as is shown in the upper panels of Figure 8.

757

## 758 **Conclusions and future prospects**

759 The work described here illuminate the conditions under which weak directional selection  
760 can interact with genetic drift to cause an increase rather than a decrease in genetic diversity  
761 at linked neutral sites. It also sheds light on the conditions under which associative  
762 overdominance rather than background selection operates. The results are, however, limited



763 in several important respects. First, only the pairwise diversity measure  $\pi$  has been studied, so  
764 that the properties of the site frequency spectra at neutral sites linked to the target of selection  
765 have not been examined; the results of Mafessoni and Lachmann (2015) and Johri *et al.*  
766 (2021) suggest that an increase in variability at a neutral locus caused by fixations of linked  
767 weakly selected mutations is accompanied by a reduction in the frequencies of rare variants  
768 relative to the standard neutral expectation. Further work is needed to investigate the  
769 magnitude and direction of distortions of the site frequency spectrum in the context of  
770 recurrent fixations and losses of weakly selected mutations. These events can cause  
771 associative overdominance, which is expected to cause a skew toward intermediate frequency  
772 variants (Becher *et al.* 2020; Gilbert *et al.* 2020).

773         Second, the extent to which multiple weakly selected loci will mutually affect each  
774 other has largely been unexplored; a recent review of relevant data suggests that such effects  
775 of multiple loci may be important for explaining the unexpectedly high levels of inbreeding  
776 depression and variation in quantitative traits in small populations (Waller 2021). Previous  
777 simulation work has shown that, with low rates of recombination and many tightly linked  
778 highly recessive or deleterious mutations, the population can “crystallize” into two  
779 haplotypes carrying complementary sets of mutations that exhibit pseudo-overdominance  
780 (Charlesworth and Charlesworth 1997; Palsson 2000; Gilbert *et al.* 2020); there is evidence  
781 for less severe effects, causing a retardation of loss of variability, when multiple loci are  
782 subject to deleterious mutations in small populations (Latter 1998; Bersabé *et al.* 2016).  
783 Further investigation of this topic is desirable. It would also be of interest to investigate the  
784 properties of subdivided populations, where stochastic effects on loci under selection can be  
785 significant when deme sizes are sufficiently small (Roze and Rousset 2004; Roze 2015;  
786 Charlesworth 2018).

787         Finally, the properties of fixation times in varying environments can be significantly  
788 different from those for a constant environment that are used here, with a breakdown in the  
789 symmetry between  $h$  and  $1 - h$  for favorable and deleterious mutations as far as  $t^*$  is  
790 concerned (Kaushik and Jain 2021). It is likely that this will also apply to times to loss. The  
791 relations of these quantities with associative overdominance in small laboratory populations  
792 will probably not be affected by this effect, but the behavior of natural populations could be  
793 significantly changed.

794

795 **Data Availability**

796 No new data or reagents were generated by this research. The codes for the computer programs  
797 used to produce the results described below will be made available on Figshare on acceptance.

798

### 799 **Conflicts of Interest**

800 None

801

### 802 **Acknowledgments**

803 I thank two anonymous reviewers, Graham Coop, Kavita Jain and Lei Zhao for their  
804 comments on the manuscript, which have helped to improve it; in particular, Lei Zhao  
805 detected errors in the original versions of Equations (3b) and (8b), which have been  
806 corrected.

807

### 808 **Literature Cited**

- 809 Assaf ZJ, Tilk S, Park J, Siegal ML, Petrov DA. 2017. Deep sequencing of natural and  
810 experimental populations of *Drosophila melanogaster* reveals biases in the spectrum of new  
811 mutations. *Genome Res.* 27:1988-2000.
- 812 Becher H, Jackson BC, Charlesworth B. 2020. Patterns of genetic variability in genomic  
813 regions with low rates of recombination. *Curr. Biol.* 30:94-100.
- 814 Bersabé D, Caballero A, Pérez-Figueroa A, García-Dorado A. 2016. On the consequences of purging  
815 and linkage on fitness and genetic diversity. *G3* 6:171-181.
- 816 Bulmer MG. 1991. The selection-mutation-drift theory of synonymous codon usage. *Genetics*  
817 129:897-907.
- 818 Campos JL, Charlesworth B. 2019. The effects on neutral variability of recurrent  
819 selective sweeps and background selection. *Genetics* 212:287-303.
- 820 Charlesworth B. 2018. Mutational load, inbreeding depression and heterosis in subdivided  
821 populations. *Mol. Ecol.* 24:4991-5003.
- 822 Charlesworth B. 2020a. How long does it take to fix a favorable mutation,  
823 and why should we care? *Am. Nat.* 195:753-771.
- 824 Charlesworth B. 2020b. How good are predictions of the effects of selective sweeps on  
825 levels of neutral diversity? *Genetics* 216:1217-1239.
- 826 Charlesworth B, Charlesworth D. 1997. Rapid fixation of deleterious alleles by Muller's ratchet.  
827 *Genet. Res.* 70:63-73.
- 828 Charlesworth B, Jensen JD. 2021. Effects of selection at linked sites on patterns of genetic  
829 variability. *Ann. Rev. Ecol. Evol. Syst.* 52:177-197.

- 830 Charlesworth B, Morgan MT, Charlesworth D. 1993. The effect of deleterious mutations on  
831 neutral molecular variation. *Genetics* 134:1289-1303.
- 832 Cutter AD, Payseur BA. 2013. Genomic signatures of selection at linked sites: unifying the  
833 disparity among species. *Nature Rev. Genet.* 14:262-272.
- 834 Ewens WJ. 2004. *Mathematical Population Genetics. 1. Theoretical Introduction*. New York:  
835 Springer.
- 836 Fisher RA. 1930. The distribution of gene ratios for rare mutations. *Proceedings of the Royal*  
837 *Society of Edinburgh* 50:205-220.
- 838 Frydenberg O. 1963. Population studies of a lethal mutant in *Drosophila melanogaster*. I.  
839 Behaviour in populations with discrete generations. *Hereditas* 50:89-116.
- 840 Gilbert KJ, Pouyet F, Escoffier L, Peischel S. 2020. Transition from background selection to  
841 associative overdominance promotes diversity in regions of low recombination. *Curr.*  
842 *Biol.* 30:101-107.
- 843 Hudson RR, Kaplan NL. 1995. Deleterious background selection with recombination.  
844 *Genetics* 141:1605-1617.
- 845 Johri P, Charlesworth B, Howell EK, Lynch M, Jensen JD. 2021. Revisiting the notion of  
846 deleterious sweeps. *Genetics* 219: iyab094.
- 847 Kaushik S, Jain K. 2021. Time to fixation in changing environments. *Genetics* 219: iyab148.
- 848 Kimura M. 1983. *The Neutral Theory of Molecular Evolution*. Cambridge: Cambridge  
849 University Press.
- 850 Kimura M. 1971. Theoretical foundations of population genetics at the molecular level.  
851 *Theor. Pop. Biol.* 2:174-208.
- 852 Kimura M, Ohta T. 1969. The average number of generations until fixation of a mutant gene  
853 in a finite population. *Genetics* 61:763-771.
- 854 Latter BDH. 1998. Mutant alleles of small effect are primarily responsible for the loss of  
855 fitness with slow inbreeding in *Drosophila melanogaster*. *Genetics* 148:1143-1158.
- 856 Li W-H. 1987. Models of nearly neutral mutations with particular implications for non-  
857 random usage of synonymous codons. *J. Mol. Evol.* 24:337-345.
- 858 Mafessoni F, Lachmann D. 2015. Selective strolls: fixation and extinction in diploids  
859 are slower for weakly selected mutations than for neutral ones. *Genetics* 201:1581-  
860 1589.
- 861 Malécot G. 1969. *The Mathematics of Heredity*. San Francisco, CA: W.H. Freeman.
- 862 Maruyama T. 1972. The average number and the variance at a particular gene frequency in  
863 the course of fixation of a mutant gene in a finite population. *Genet. Res.* 19:109-114.

- 864 Maruyama T, Kimura M. 1974. A note on the speed of gene frequency changes in reverse  
865 directions in a finite population. *Evolution* 28:161-163.
- 866 McVean GAT, Charlesworth B. 1999. A population genetic model for the evolution of synonymous  
867 codon usage: patterns and predictions. *Genet. Res.* 74:145-158.
- 868 Moinet, A, Peischl, S, and Excoffier, L. 2021. Strong neutral sweeps occurring during a population  
869 contraction. *BioRxiv* 10.1101/2021.08.25.457712.
- 870 Nordborg M, Charlesworth B, Charlesworth D. 1996. The effect of recombination on  
871 background selection. *Genet. Res.* 67:159-174.
- 872 Ohta T. 1971. Associative overdominance caused by linked detrimental mutations. *Genet.*  
873 *Res.* 18:277-286.
- 874 Palsson S. 2001. The effects of deleterious mutations in cyclically parthenogenetic organisms. *J.*  
875 *Theor. Biol.* 208:201-214.
- 876 Palsson S, Pamilo P. 1999. The effects of deleterious mutations on linked neutral variation in  
877 small populations. *Genetics* 153:475-483.
- 878 Pamilo P, Palsson S. 1998. Associative overdominance, heterozygosity and fitness. *Heredity*  
879 81:381-389.
- 880 Roze D. 2015. Effects of interference between selected loci on the mutation load, inbreeding  
881 depression and heterosis. *Genetics* 201:745-757.
- 882 Roze D, Rousset F. 2004. Joint effects of self-fertilization and population structure on mutation load,  
883 inbreeding depression and heterosis. *Genetics* 167:1001-101.
- 884 Schou MF, V. L, Bechsgaard J, Schlötterer C, Kristensen TN. 2017. Unexpected high  
885 diversity in small populations suggests maintenance by associative overdominance.  
886 *Mol. Ecol.* 26:6510-6523.
- 887 Sved JA. 1968. The stability of linked systems of loci with a small population size. *Genetics*  
888 59:543-563.
- 889 Tajima F. 1990. Relationship between DNA polymorphism and fixation time. *Genetics*  
890 125:447-454.
- 891 Waller DM. 2021. Addressing Darwin's dilemma: Can pseudo-overdominance explain  
892 persistent inbreeding depression and load? *Evolution* 75:779-793.
- 893 Wang J, Hill WG. 1999. Effect of selection against deleterious mutations on the decline in  
894 heterozygosity at neutral loci in closely inbreeding populations. *Genetics* 153:1475-  
895 1489.
- 896 Wiehe THE, Stephan W. 1993. Analysis of a genetic hitchhiking model and its application to  
897 DNA polymorphism data. *Mol. Biol. Evol.* 10:842-854.

898 Zhao L, Charlesworth B. 2016. Resolving the conflict between associative  
899 overdominance and background selection. *Genetics* 203:1315-1334.  
900

901 **Appendix**

902 **Conditional sojourn time formulae**

903 Equation (4.52) of Ewens (2004) can be used to evaluate the sojourn time density conditional on  
904 fixation for an allele  $A_2$  at frequency whose initial frequency is  $q = 1/N_H$ , so that  $x \geq q$ . This  
905 equation can be rewritten as:

906

907 
$$t^*(x, q) = 2P_1(x)[x(1-x)\psi(x)]^{-1} \int_x^1 \psi(y) dy \quad (\text{A1a})$$

908

909 where  $P_1(x)$  is the probability of fixation from frequency  $x$ , respectively, which is given by:

910

911 
$$P_1(x) = \int_0^x \psi(y) dy / \int_0^1 \psi(y) dy \quad (\text{A1b})$$

912

913 
$$\psi(y) = \exp - 2 \int \frac{\Delta y}{y(1-y)} dy \quad (\text{A1c})$$

914

915 Similarly, the probability of loss from frequency  $x$  is given by:

916

917 
$$P_0(x) = \int_x^1 \psi(y) dy / \int_0^1 \psi(y) dy \quad (\text{A1d})$$

918

919 (Ewens 2004, Equations 4.15-4.17).

920 Substituting the expression for  $\Delta x$  given by Equation (1) of the main text into Equation  
921 (A1c) we have:

922 
$$\psi(y) = \exp - \gamma(2ay + by^2) \quad (\text{A2})$$

923

924 For  $b = 0$  (semi-dominance) analytic expressions for the integrals in Equations (A1) are  
925 available (Ewens 2004, pp.165, 169 -170). In other cases, numerical evaluations are needed if the  
926 approximations derived below are to be avoided. For this purpose, it is convenient to use series  
927 representations of the integrals in Equations (A1b) and (A1c). Expanding the exponential function  
928 in Equation (A2), the indefinite integral of  $\psi(y)$  can be written as:

929

930 
$$\int \psi(y) dy = 1 + \sum_{i=1}^{\infty} \frac{(-\gamma)^i}{i!} \int (2ay + by^2)^i dy \quad (\text{A3a})$$

931

932 With  $b \neq 0$ , and writing  $c = a/b$ , this expression can be reduced to a simpler form by the  
 933 transform  $z = (y + c)\sqrt{|\gamma b|}$ , which gives  $\psi(y)dy = \exp(\gamma ac)\exp(-z^2) dz/\sqrt{|\gamma b|}$  if  $\gamma b > 0$   
 934 and  $\exp(\gamma ac)\exp(z^2) dz/\sqrt{|\gamma b|}$  if  $\gamma b < 0$ . The terms in  $\exp(-z^2)$  or  $\exp(z^2)$  can then be  
 935 expanded as a Taylor series in  $z$ , and integrated term by term to yield an infinite series in  $z$ :

936  
 937 
$$\sqrt{|\gamma b|} \int \psi(y) dy = \exp(\gamma ac) \sum_{i=0}^{\infty} \frac{(-1)^i z^{2i+1}}{(2i+1)!} \quad (\gamma b > 0) \quad (\text{A3b})$$

938 
$$\sqrt{|\gamma b|} \int \psi(y) dy = \exp(\gamma ac) \sum_{i=0}^{\infty} \frac{z^{2i+1}}{(2i+1)!} \quad (\gamma b < 0) \quad (\text{A3c})$$

939

940 If third- and higher-order terms in  $\gamma$  in Equations (A1) - (A3a) are neglected, the following  
 941 approximations for the components of Equations (A1) emerge after some algebra:

942

943 
$$\psi(x)^{-1} \approx 1 + \gamma(2ax + bx^2) + \gamma^2(2a^2x^2 + 2abx^3 + \frac{1}{2}b^2x^4) \quad (\text{A4a})$$

944

945 
$$\int_0^x \psi(y) dy \approx x \left[ 1 - \gamma(ax + \frac{1}{3}bx^2) + \gamma^2 \left( \frac{2}{3}a^2x^2 + \frac{1}{2}abx^3 + \frac{1}{10}b^2x^4 \right) \right] \quad (\text{A4b})$$

946

947 
$$\int_0^1 \psi(y) dy^{-1} \approx 1 + \gamma(a + \frac{1}{3}b) + \gamma^2 \left( \frac{1}{3}a^2 + \frac{1}{6}ab + \frac{1}{90}b^2 \right) \quad (\text{A4c})$$

948

949 
$$\int_x^1 \psi(y) dy \approx (1-x) \left\{ 1 - \gamma \left[ a(1+x) + \frac{1}{3}b(1+x+x^2) \right] + \gamma^2 \left[ \frac{2}{3}a^2(1+x+x^2) + \right. \right.$$
  
 950 
$$\left. \frac{1}{2}ab(1+x+x^2+x^3) + \frac{1}{10}b^2(1+x+x^2+x^3+x^4) \right\} \quad (\text{A4d})$$

951

952 Inserting these expressions into Equation (A1a), and neglecting higher-order terms in  $\gamma$ , we  
 953 obtain:

954 
$$t^*(x, q) \approx 2 \left\{ 1 - \frac{1}{3}\gamma bx(1-x) - \frac{1}{3}\gamma^2 x(1-x) \left[ a^2 + \frac{1}{2}ab(1+2x) \right. \right.$$
  

$$\left. \left. + \frac{1}{30}b^2(1+x[2+13x]) \right] \right\} \quad (\text{A5})$$

955

956 For the sojourn time density conditional on loss, Equation (4.52) of Ewens (2004) can be  
 957 used:

958 
$$t^{**}(x, q) = 2 \left[ \int_x^1 \psi(y) dy \right]^2 P_1(q) [P_0(q)x(1-x)\psi(x) \int_0^1 \psi(y) dy]^{-1} \quad (\text{A6})$$

959

960 Using the procedure applied to  $t^*(x, q)$ , the following second-order approximation with  
 961 respect to  $\gamma$  is obtained:

962

$$963 \quad t^{**}(x, N_H^{-1}) \approx 2N_H^{-1}(1-x)x^{-1}\left\{1 - \frac{1}{3}\gamma bx(2-x) - \frac{1}{3}\gamma^2 x[a^2(2-x) + ab(1+x[1-x])]\right. \\ 964 \quad \left. + \frac{1}{30}b^2(x + [2-3x][1-3x] + 13x^2[1-x])\right\} \quad (A7)$$

965

966 An approximation for the density function for the expected sojourn time between loss or  
 967 fixation at frequency  $x$  for a new mutation can similarly be obtained from Equation (4.23) of Ewens  
 968 (2004):

$$969 \quad t(x, N_H^{-1}) \approx 2N_H^{-1} \int_x^1 \psi(y) dy [x(1-x)\psi(x) \int_0^1 \psi(y) dy]^{-1} \quad (A8)$$

970

971 This expression yields:

972

$$973 \quad t(x, N_H^{-1}) \approx 2N_H^{-1}x^{-1}\left\{1 + \gamma x \left[ a - \frac{1}{3}b(1-2x) \right] - \frac{1}{3}\gamma^2 x[a^2(1-2x) + \right. \\ 974 \quad \left. \frac{1}{2}ab(1+x[3-5x]) + \frac{1}{30}b^2(1+x[1+x(21-24x)])\right\} \quad (A9)$$

975

### 976 **Background selection approximation**

977 In this case, only losses of new mutations to the deleterious allele  $A_2$  from a population fixed for the  
 978 favorable allele  $A_1$  need to be considered. It is assumed that this process has been going on  
 979 indefinitely, and that the population is being observed over a long time period  $T_o$  (in units of  $2N_e$   
 980 generations); the mean diversity at the neutral site is then taken over this period. From Table 1, the  
 981 expected number of losses of  $A_2$  over this period is  $\lambda_{10}T_o = 0.5\theta_s N_H P_{10}T_o$ , and the expected time  
 982 interval between successive losses is  $T_l = 1/\lambda_{10}$ , where  $T_l \ll 1$  in the case of BGS. At the start of  
 983 this process, which can be assumed to have occurred long before the period of observation, there is  
 984 a deviation  $\Delta\pi_{2l}$  from 1 of the relative diversity at the end of the first loss event (see Table 1), whose  
 985 value can be found by the simulation procedure described in the main text. This is followed by a  
 986 recovery period, whose length is drawn from an exponential distribution with rate parameter  $\lambda_{10}$ , so  
 987 that the new expected value of  $\Delta\pi$  at the end of the recovery period is:

988

$$989 \quad \Delta\pi_{2l}^* = \Delta\pi_{2l} \lambda_{10} \int_0^\infty \exp[-(1 + \lambda_{10})t] dt = \frac{\Delta\pi_{2l} \lambda_{10}}{(1 + \lambda_{10})} \approx \Delta\pi_{2l} \exp(-T_l) \quad (A10)$$

990



991 The sum of the  $\Delta\pi$  values over the recovery period is approximately equal to  $\Delta\pi_{2l}T_l$ , since  
992 most values will be close to  $\Delta\pi_{2l}$  due to the short length of this period; a more exact derivation of  
993 this result can be obtained by use of the argument that yielded Equation S22 of Campos and  
994 Charlesworth (2019).

995 If the change in diversity at each event is small, we can assume additivity of individual  
996 effects in order to obtain the net change after several events. The second loss event thus results in a  
997 deviation before recovery of  $\Delta\pi_{2l}^* + \Delta\pi_{2l}$  and a corresponding sum of  $\Delta\pi$  over the recovery period  
998 of  $(\Delta\pi_{2l}^* + \Delta\pi_{2l})T_l$ . Using the argument above, the post-recovery deviation  $\approx$   
999  $(\Delta\pi_{2l}^* + \Delta\pi_{2l})\exp(-T_l) = \Delta\pi_{2l}[1 + \exp(-T_l)]\exp(-T_l)$ , and the corresponding sum of  $\Delta\pi$  values  
1000 over the recovery period  $\approx \Delta\pi_{2l}[1 + \exp(-T_l)]T_l$ . If this process is repeated indefinitely, it can be  
1001 seen that the individual post-recovery deviations are given by the product of  $\Delta\pi_{2l}\exp(-T_l)$  and the  
1002 sum of a geometric series in  $\exp(-T_l)$ , which converges on:

1003

$$1004 \quad \Delta\pi_{2l} \exp(-T_l) / [1 - \exp(-T_l)] \approx \Delta\pi_{2l} \lambda_{10} \quad (\text{A11a})$$

1005

1006 Similarly, the sum of the individual deviations over the recovery period converges on:

1007

$$1008 \quad \Delta\pi_{2l} \lambda_{10} T_l = \Delta\pi_{2l} \quad (\text{A11b})$$

1009

1010

1011 This formula is the same as for the case when there is a complete recovery of diversity after a  
1012 loss of  $A_2$ . It therefore follows that the net deviation in diversity caused by multiple losses of  
1013  $A_2$  at rate  $\lambda_{10}$  is approximated by:

1014

$$1015 \quad \lambda_{10} (\Delta\pi_{20w} + \Delta\pi_{2l}) \quad (\text{A12})$$

1016

1017 **Table 1 Parameters used in the model of associative overdominance**

1018

1019	$u$	rate of mutation per generation from $A_1$ to $A_2$ at the selected locus
1020	$v$	rate of mutation per generation from $A_2$ to $A_1$ at the selected locus
1021	$\kappa$	mutational bias parameter, such that $u = \kappa v$
1022	$\theta_s$	scaled mutation rate at the selected locus, such that $\theta_s = 4N_e u$
1023	$P_{10}$	Probability of loss of an $A_2$ mutation introduced into a population fixed for $A_1$ .
1024	$P_{11}$	Probability of fixation of an $A_2$ mutation introduced into a population fixed for $A_1$ .
1025	$P_{20}$	Probability of loss of an $A_1$ mutation introduced into a population fixed for $A_2$ .
1026	$P_{21}$	Probability of fixation of an $A_1$ mutation introduced into a population fixed for $A_2$ .
1027	$\lambda_{10}$	Rate of loss of new $A_2$ mutations from a population fixed for $A_1$ (in units of $2N_e$
1028		generations); $\lambda_{10} = 0.5\theta_s N_H P_{10}$
1029	$\lambda_{11}$	Rate of fixation of new $A_2$ mutations in a population fixed for $A_1$ (in units of $2N_e$
1030		generations); $\lambda_{11} = 0.5\theta_s N_H P_{11}$
1031	$\lambda_{20}$	Rate of loss of new $A_1$ mutations from a population fixed for $A_2$ (in units of $2N_e$
1032		generations); $\lambda_{20} = 0.5\kappa^{-1}\theta_s N_H P_{20}$
1033	$\lambda_{21}$	Rate of fixation of new $A_1$ mutations in a population fixed for $A_2$ (in units of $2N_e$
1034		generations); $\lambda_{21} = 0.5\kappa^{-1}\theta_s N_H P_{21}$
1035	$\Delta\pi_{il}$	Value of $\Delta\pi$ at the neutral site, when an allele of type $A_i$ has just become lost from the
1036		linked selected site.
1037	$\Delta\pi_{if}$	Value of $\Delta\pi$ at the neutral site, when an allele of type $A_i$ has just become fixed at the
1038		linked selected site.
1039	$\Delta\pi_{0S}$	Sum of $\Delta\pi$ values at the neutral site over the course of the loss of a type $i$ mutation from the
1040		linked selected site.
1041	$\Delta\pi_{1S}$	Sum of $\Delta\pi$ values at the neutral site over the course of the fixation of a type $i$ mutation at the
1042		linked selected site.
1043		

1044 **Table 2 Comparison of the deterministic BGS predictions for the**  
1045 **reduction in neutral diversity with simulations of losses of**  
1046 **deleterious mutations from populations fixed for the favorable allele**

$h$	$u/hs = 0.2$	$u/hs = 0.1$	$u/hs = 0.05$	$u/hs = 0.025$
0.4	$\gamma = 6.25$ 0.124±0.011	$\gamma = 12.5$ 0.089±0.003	$\gamma = 25$ 0.053±0.001	$\gamma = 50$ 0.027±0.001
0.3	$\gamma = 8.33$ 0.130±0.005	$\gamma = 16.6$ 0.084±0.003	$\gamma = 33.3$ 0.050±0.001	$\gamma = 66.6$ 0.027±0.001
0.2	$\gamma = 2.5$ 0.123±0.005	$\gamma = 25$ 0.076±0.002	$\gamma = 50$ 0.035±0.001	$\gamma = 100$ 0.026±0.001
0.1	$\gamma = 25$ 0.102±0.003	$\gamma = 50$ 0.066±0.002	$\gamma = 100$ 0.041±0.001	$\gamma = 200$ 0.024±0.001

1047

1048

1049 The lower entries in each cell are the simulation results for the reductions in neutral diversity  
1050 (with standard errors) under recurrent losses of completely linked, deleterious mutant alleles  
1051 from a population fixed for the selectively favorable alternative, with mutation rate  $u$  to  
1052 deleterious alleles, selection coefficient  $s$  and dominance coefficient  $h$ . The population size is  
1053  $N = 500$ , so that  $s = \gamma/1000$ , the scaled deleterious mutation rate is  $\theta_s = 4Nu = 1$ , and  $u = 2.5 \times$   
1054  $10^{-4}$ .

1055

1056

1057

1058 Figure 1. Mean time to fixation of a new mutation as a function of the absolute value of the

1059 scaled selection coefficient  $\gamma$ , assuming autosomal inheritance and a Wright-Fisher model of

1060 genetic drift with population size  $N$ . Times are in units of coalescent time ( $2N$  generations).

1061 The cases with negative selection have a dominance coefficient  $h = 0.1$  and those with

1062 positive selection have  $h = 0.9$ . The results for two different values of  $N$  are shown. The red

1063 points with error bars are the mean values from simulations and their standard errors. The

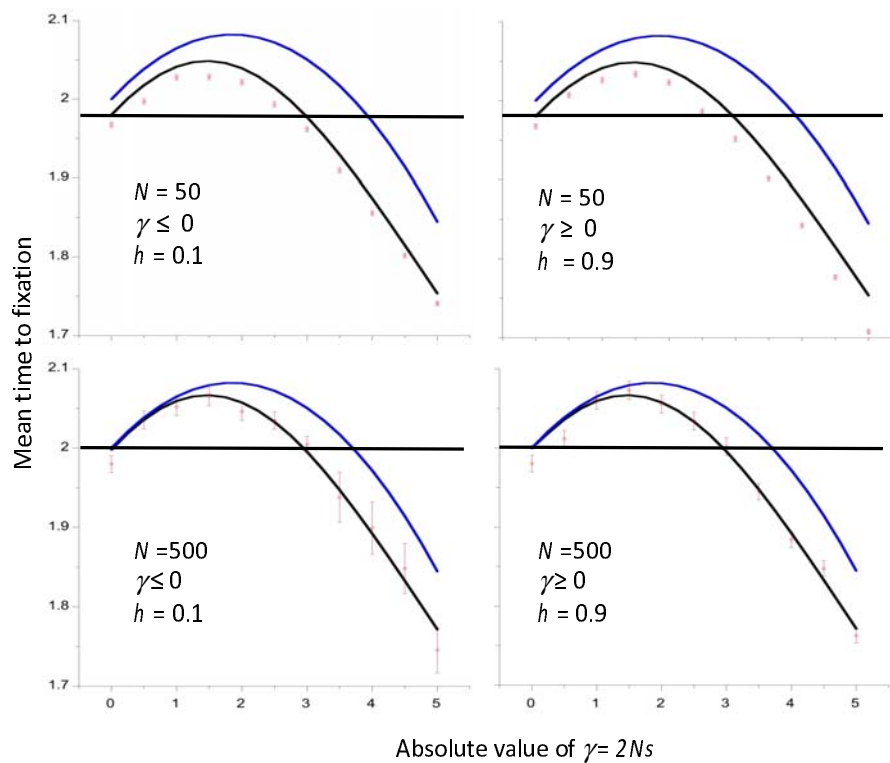
1064 blue curves are the values from the approximation of Equation (2), and the black curves are

1065 the values from numerical integrations of the diffusion equation results (Equations A1). The

1066 horizontal lines are the neutral values from the numerical integrations.

1067

1068



1069

1070

1071

1072

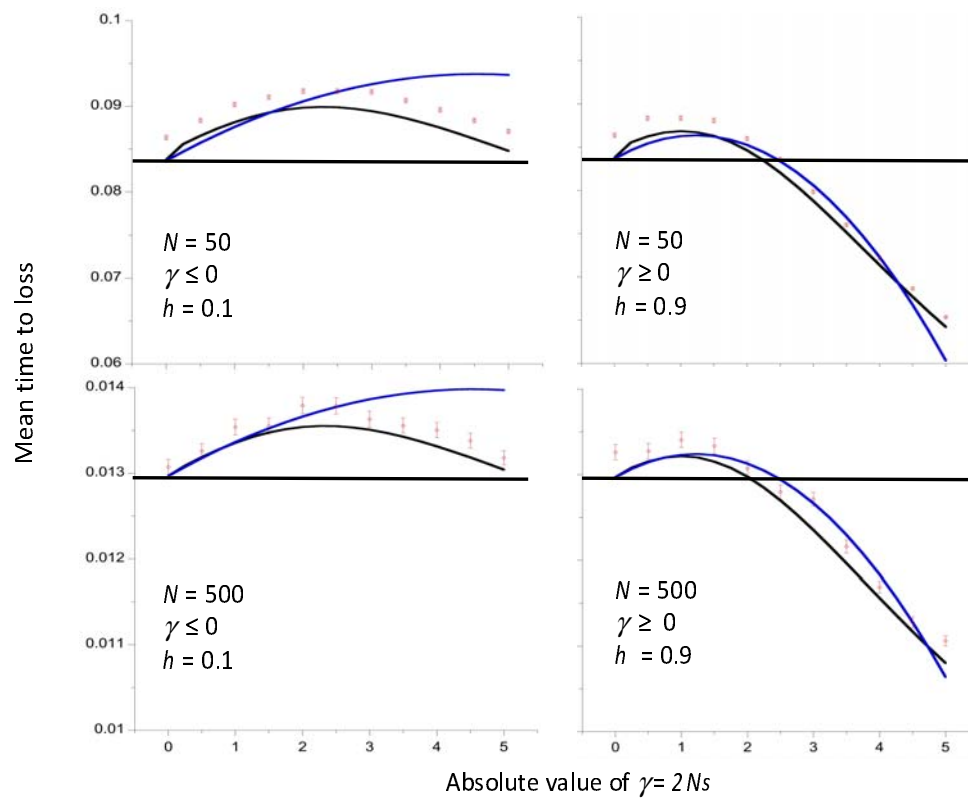
1073

1074

1075 Figure 2. Mean time to loss of a new mutation as a function of the absolute value of the  
1076 scaled selection coefficient, assuming autosomal inheritance and a Wright-Fisher model of  
1077 genetic drift with population size  $N$ . Times are in units of coalescent time ( $2N$  generations).  
1078 The cases with negative selection have a dominance coefficient  $h = 0.1$  and those with  
1079 positive selection have  $h = 0.9$ . The results for two different values of the population size,  $N$ ,  
1080 are shown. The red points with error bars show the mean values of simulations and their  
1081 standard errors. The blue curves are the values from the approximation of Equation (3), and  
1082 the black curves are the values from numerical integrations of the diffusion equation results  
1083 (Equations A1 and A6). The horizontal lines are the neutral values from the numerical  
1084 integrations.

1085

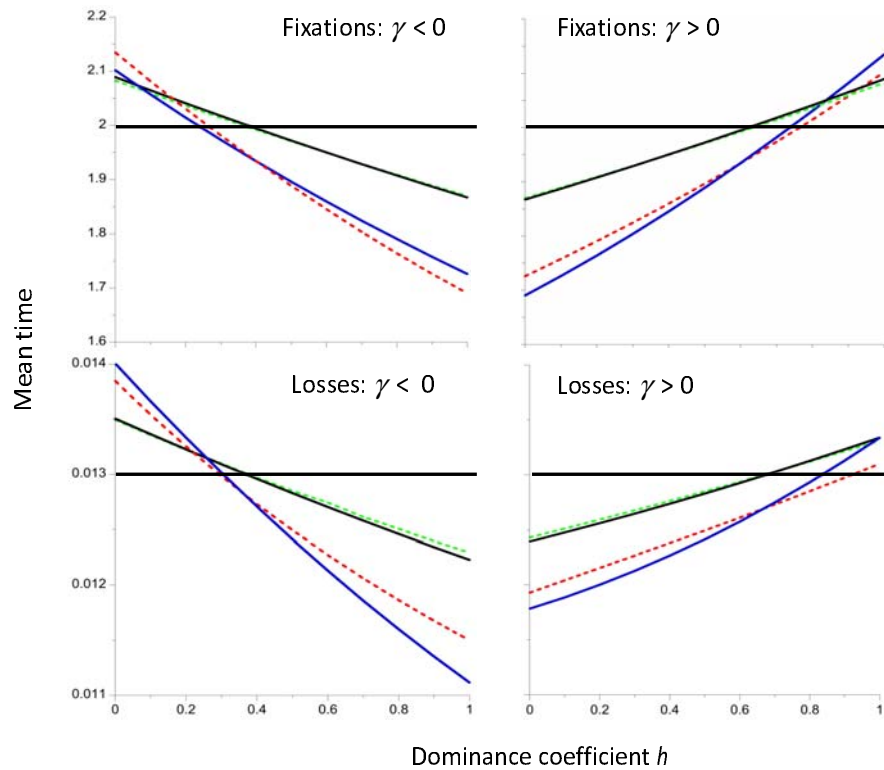
1086



1087

1088

1089 Figure 3. Mean time to fixation and loss of a new mutation (in units of coalescent time) as a  
1090 function of the dominance coefficient  $h$ , for the models used in Figures 1 and 2. The black  
1091 and blue lines use the approximations of Equations (2) and (3) to generate results for  $|\gamma| = 1$   
1092 and 2, respectively. The dashed green and red lines are the corresponding values from  
1093 numerical integrations of the diffusion equation expressions. The horizontal lines are the  
1094 neutral values from the numerical integrations. The population size  $N$  is equal to 500.  
1095



1096  
1097

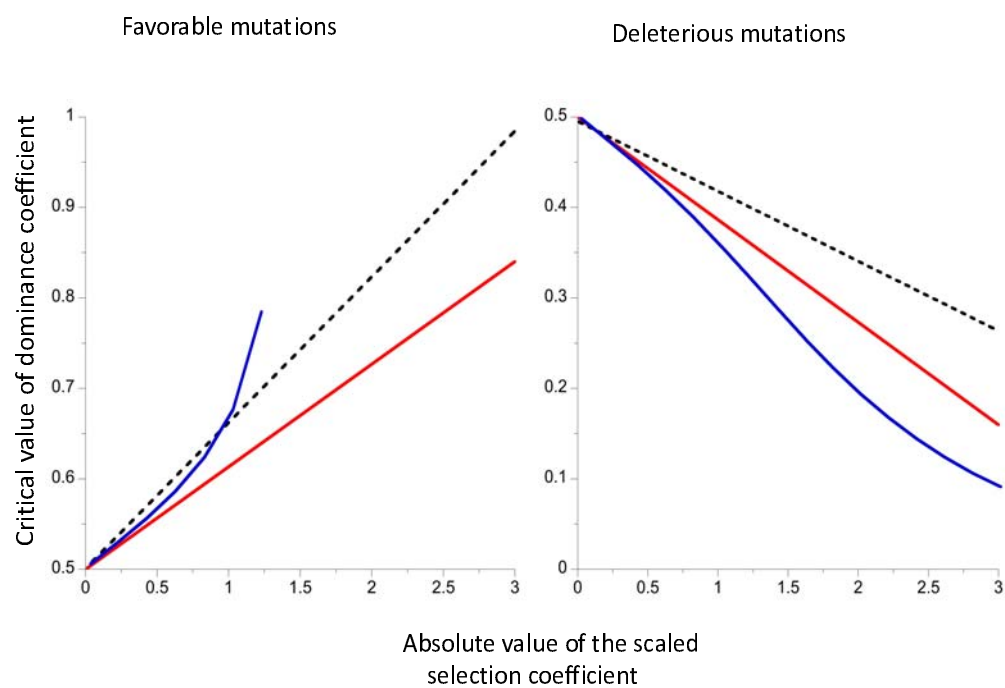
1098

1099

1100 Figure 4. The critical values of the dominance coefficient as functions of the scaled selection  
1101 coefficient for mean fixation time (full red line) or mean loss time (dashed black line). The  
1102 results were obtained using the approximate Equations (8). The blue curves are the  
1103 solutions to Equation (18) of Zhao and Charlesworth (2016). The results for favorable  
1104 mutations are shown in the left-hand panel) and those for deleterious mutations in the  
1105 right-hand panel

1106

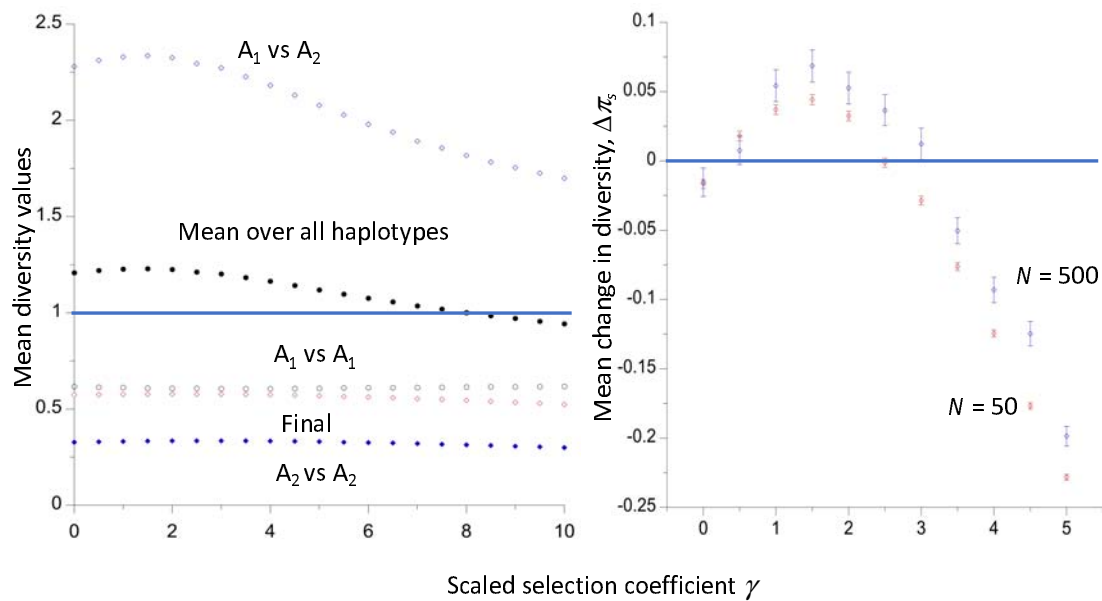
1107



1108

1109

1110 Figure 5. The left-hand panel shows the mean pairwise diversities (relative to the purely  
1111 neutral value  $\theta$ ) at a neutral site during the course of fixation of a completely linked  
1112 beneficial mutation with dominance coefficient  $h = 0.9$ , for haplotypes carrying the  
1113 ancestral allele ( $A_1$ ), the new mutation ( $A_2$ ), and the divergence between  $A_1$  and  $A_2$   
1114 haplotypes ( $A_1$  versus  $A_2$ ). The final diversity at the time of fixation of  $A_2$ , and the mean  
1115 diversity over all three haplotypes over the course of the fixation process, are also shown.  
1116 Autosomal inheritance and a Wright-Fisher model of genetic drift with population size  $N =$   
1117 50 were simulated by the method of Tajima (1990). The right-hand panel displays the mean  
1118 values and standard errors of the net change in relative diversity over repeated fixation  
1119 events for two different  $N$  values, estimated from the simulations by the method described  
1120 in the text.  
1121



1122  
1123

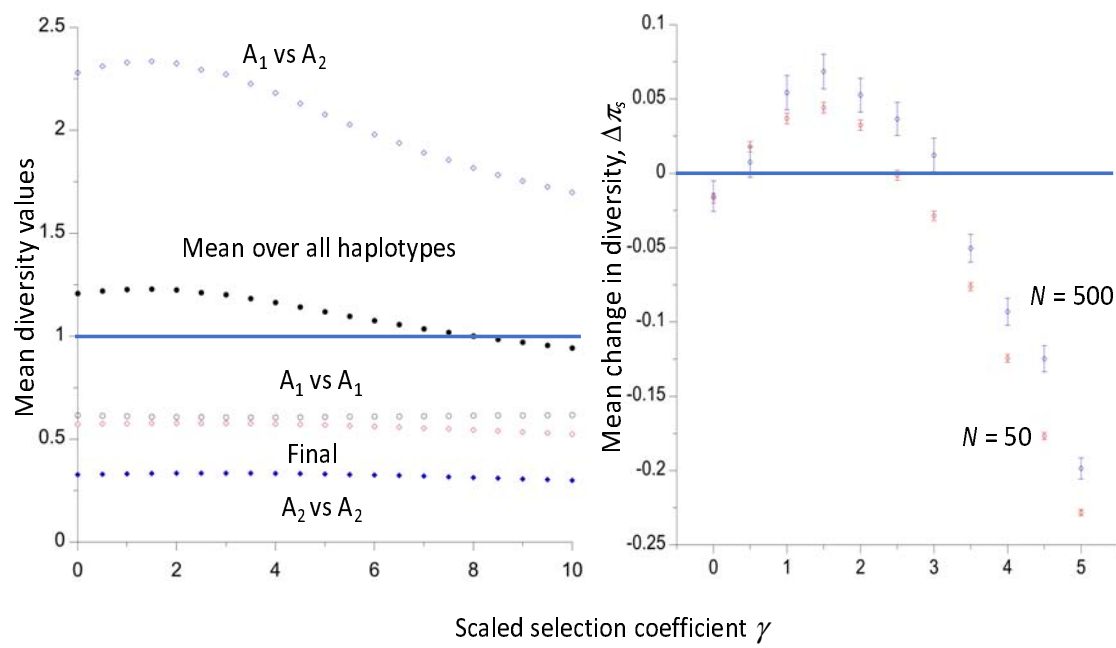


1124 Figure 6. The mean values and standard errors of the net changes in relative diversity over  
1125 repeated loss events with two different  $N$  values, for deleterious mutations with  $h = 0.1$  and  
1126 favorable mutations with  $h = 0.9$ , using the same model and methods as in Figure 7.

1127

1128

1129



1130

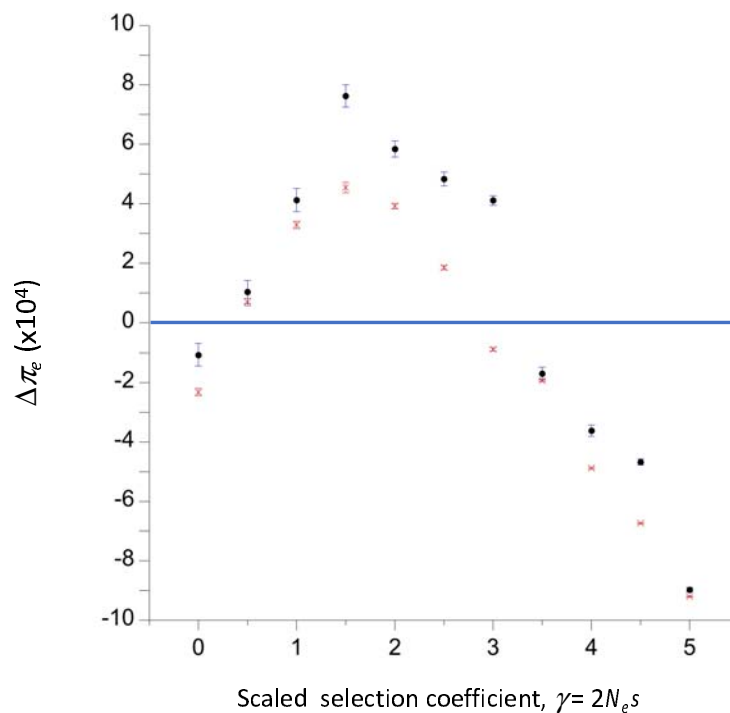
1131

1132 Figure 7. The expected deviation of relative diversity for a completely linked neutral site  
1133 from its value in the absence of selection ( $\Delta\pi_e$ ), at the stationary state under genetic drift,  
1134 mutation and selection. The dominance coefficients for deleterious and favorable mutations  
1135 are  $h = 0.1$  and  $h = 0.9$ , respectively. Equal frequencies of mutations in each direction at the  
1136 selected site were assumed, with a scaled mutation rate  $\theta_s = 0.01$ . The means and standard  
1137 errors over replicate simulations are shown for population sizes of 50 (red points) and 500  
1138 (black points).

1139

1140

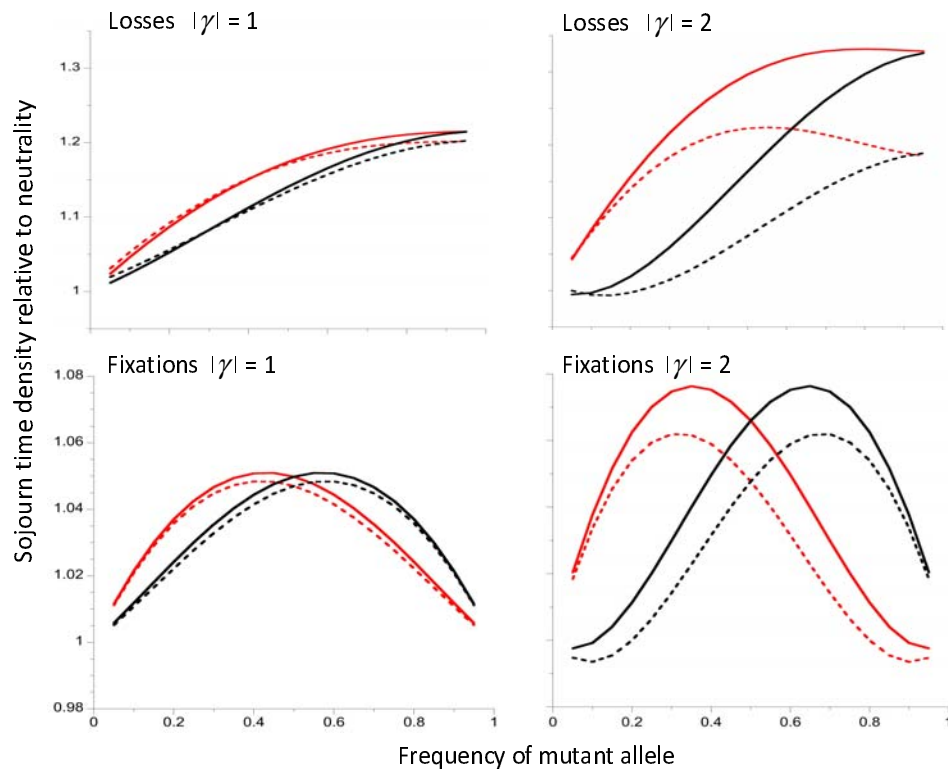
1141



1142

1143

1144 Figure 8. The upper two panels show the approximate (full curves) and exact (dashed  
1145 curves) sojourn time densities for mutations that become lost, relative to the corresponding  
1146 neutral values. The lower two panels are the sojourn time densities for mutations that  
1147 become fixed. The left-hand panels are for  $|\gamma| = 1$  and the right-hand panels are for  $|\gamma| = 2$ .  
1148 Deleterious mutations with  $h = 0.1$  are the red curves and beneficial mutations with  $h = 0.9$   
1149 are the black curves. The exact results were obtained by numerical integrations of the  
1150 relevant equations described in the Appendix; the approximate results were obtained from  
1151 Equations (A5) and (A7).  
1152



1153  
1154  
1155  
1156  
1157